Classification of reflection-symmetry-protected topological semimetals and nodal superconductors

Ching-Kai Chiu[1,2,*] and Andreas P. Schnyder[3,†]

[1]*Department of Physics and Astronomy, University of British Columbia, Vancouver, BC, Canada V6T 1Z1*

[2]*Quantum Matter Institute, University of British Columbia, Vancouver BC, Canada V6T 1Z4*

[3]*Max-Planck-Institut für Festkörperforschung, Heisenbergstrasse 1, D-70569 Stuttgart, Germany*

(Received 29 August 2014; revised manuscript received 12 November 2014; published 26 November 2014)

While the topological classification of insulators, semimetals, and superconductors in terms of nonspatial symmetries is well understood, less is known about topological states protected by crystalline symmetries, such as mirror reflections and rotations. In this work, we systematically classify topological semimetals and nodal superconductors that are protected, not only by nonspatial (i.e., global) symmetries, but also by a crystal reflection symmetry. We find that the classification crucially depends on (i) the codimension of the Fermi surface (nodal line or point) of the semimetal (superconductor), (ii) whether the mirror symmetry commutes or anticommutes with the nonspatial symmetries, and (iii) how the Fermi surfaces (nodal lines or points) transform under the mirror reflection and nonspatial symmetries. The classification is derived by examining all possible symmetry-allowed mass terms that can be added to the Bloch or Bogoliubov–de Gennes Hamiltonian in a given symmetry class and by explicitly deriving topological invariants. We discuss several examples of reflection-symmetry-protected topological semimetals and nodal superconductors, including topological crystalline semimetals with mirror $\mathbb{Z}_2$ numbers and topological crystalline nodal superconductors with mirror winding numbers.

DOI: 10.1103/PhysRevB.90.205136 PACS number(s): 03.65.Vf, 74.50.+r, 73.20.Fz

I. INTRODUCTION

Inspired by the recent experimental discovery of two- and three-dimensional topological insulators [1–5], a multitude of novel topological states protected by different symmetries has been predicted over the last few years [4,6–9]. One of the main hallmarks of these topological materials is the appearance of protected zero-energy surface states, which arise as a consequence of the nontrivial topological characteristics of the bulk wave functions. For fully gapped topological phases protected by general nonspatial symmetries, a complete classification, the tenfold way, has been obtained for arbitrary dimensions [6–9]. This scheme classifies fully gapped noninteracting systems in terms of nonspatial symmetries, i.e., symmetries that act locally in position space, namely, time-reversal symmetry (TRS), particle-hole symmetry (PHS), and chiral or sublattice symmetry (SLS).

However, over the last few years it has become apparent that besides nonspatial symmetries, also crystalline symmetries, i.e., symmetries that act nonlocally in position space, can lead to nontrivial topological properties of bulk insulating states [10–27]. A prime example of a topological material protected by a crystalline symmetry is the topological crystalline insulator SnTe [28–31]. This band insulator exhibits Dirac-cone surface states that are protected by a mirror reflection symmetry of the crystal. Other than reflection symmetry, inversion [22–26] and rotation [17,19,27] can also give rise to topologically nontrivial quantum states of matter. In fact, it is expected that for any given discrete space-group symmetry, there is a distinct topological classification of band insulators and fully gapped superconductors, and that each of these space-group-symmetry-protected topological states can be characterized in terms of an associated crystalline topological number.

Parallel to these developments, the concept of topological band theory has been extended to semimetals with Fermi points or Fermi lines, and nodal superconductors with point nodes or line nodes [26,32–44]. Although a global topological number cannot be defined for these gapless systems, it is nevertheless possible to determine their topological characteristics and the stability of their Fermi points or Fermi lines in terms of momentum-dependent topological numbers. Notable examples of gapless topological states include Weyl semimetals [45–53], Weyl superconductors [54–57], and nodal noncentrosymmetric superconductors [58–65]. Similar to fully gapped topological materials, the topological characteristics of gapless topological states manifest themselves at the surface in the form of either linearly dispersing boundary modes (i.e., Dirac or Majorana states) or dispersionless states, forming two-dimensional surface flat bands or one-dimensional surface arcs. While a complete topological classification of semimetals and nodal superconductors in terms of nonspatial symmetries has been established recently [26,33–35], the characterization of gapless topological materials protected by crystalline symmetries has remained an open problem.

In this paper, we present a complete classification of topological semimetals and nodal superconductors protected by crystal reflection symmetries and possibly one or two nonspatial (i.e., global) symmetries. We find that the topological classification of these reflection-symmetry-protected gapless states sensitively depends on (i) the codimension of the Fermi surface, (ii) whether the reflection symmetry commutes or anticommutes with the nonspatial symmetries, and (iii) whether the Fermi points or Fermi lines are left invariant by the mirror symmetry or the nonspatial symmetries. The outcome of this classification scheme is summarized in Tables II and III, which constitute the main results of this paper. Similar to the tenfold classification in terms of nonspatial symmetries [6–9], these tables exhibit twofold and eightfold Bott periodicities as a function of spatial dimension. Two complementary methods are used to derive these classification tables. The first approach

*chiu7@phas.ubc.ca

†a.schnyder@fkf.mpg.de

is based on classifying all possible symmetry-allowed mass terms that can be added to the Bloch or Bogoliubov–de Gennes (BdG) Hamiltonian in a given symmetry class. The second method relies on the explicit derivation of different types of topological invariants that guarantee the stability of the Fermi surfaces (superconducting nodes). In order to illustrate the new topological phases predicted by these classification schemes, we discuss several specific examples of reflection-symmetry-protected topological semimetals and nodal superconductors (see Sec. IV).

The remainder of this paper is organized as follows. In Sec. II, we briefly review the classification of gapless topological materials in terms of nonspatial symmetries. This is followed by the derivation of the topological classification of reflection-symmetry-protected semimetals and nodal superconductors in Sec. III, which is the principal result of this paper. We present some explicit examples of topological semimetals and nodal superconductors protected by reflection symmetries in Sec. IV and conclude with a brief summary in Sec. V. Some technical details have been relegated to appendices.

II. GAPLESS TOPOLOGICAL MATERIALS PROTECTED BY NONSPATIAL SYMMETRIES

Since the classification of reflection-symmetry-protected topological semimetals and nodal superconductors is closely related to the topological classification of gapless states protected by global symmetries, we first briefly review the tenfold classification of gapless topological materials (cf. Appendix A). This brief review also aims to clarify some open questions which recently arose in the literature [26,33–35]. The tenfold scheme classifies gapless fermionic systems in terms of three fundamental global symmetries, i.e., antiunitary time-reversal and particle-hole symmetry, as well as chiral (i.e., sublattice) symmetry [66,67]. In momentum space, TRS and PHS of the Bloch or BdG Hamiltonian $H(\mathbf{k})$ are implemented by antiunitary operators T and C, which act on $H(\mathbf{k})$ as

$$T^{-1}H(-\mathbf{k})T = +H(\mathbf{k}) \text{ and } C^{-1}H(-\mathbf{k})C = -H(\mathbf{k}), \quad (1)$$

respectively. Both T and C can square either to $+1$ or -1, depending on the type of the symmetry (see last three columns of Table I). Chiral symmetry, on the other hand, is implemented by

$$S^{-1}H(\mathbf{k})S = -H(\mathbf{k}), \quad (2)$$

where S is a unitary operator.

A. Tenfold classification of gapless topological materials

As it turns out, the topological classification of gapless materials depends not only on the symmetry class of the Hamiltonian and the codimension p of the Fermi surface

$$p = d - d_{\mathrm{FS}}, \quad (3)$$

where d and d_{FS} denote the dimension of the Brillouin zone (BZ) and the Fermi surface, respectively, but also on how the Fermi surface transforms under the global symmetries [33]. Regarding the symmetry properties of the Fermi surfaces, two different cases have to be distinguished: (i) each individual Fermi surface is left invariant under nonspatial symmetries, and (ii) different Fermi surfaces are pairwise related to each other by nonspatial symmetries (see Fig. 1). While most of the recent literature has studied case (i) [26,34,35], we emphasize that also in case (ii) there exist topologically stable Fermi surfaces.

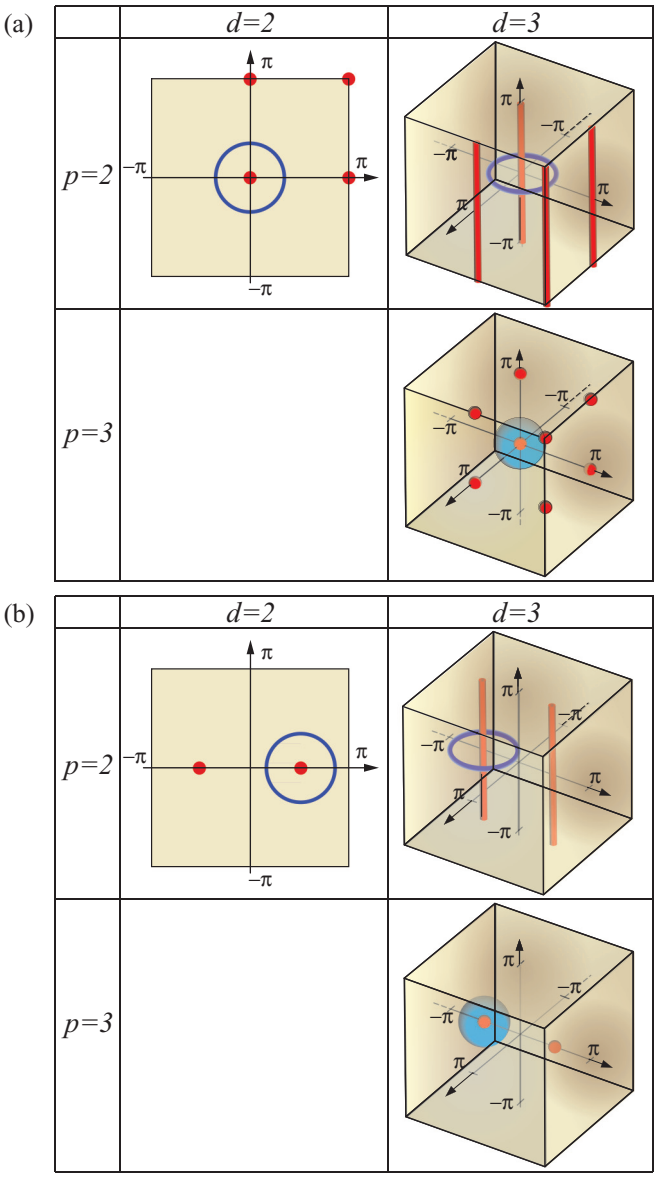

FIG. 1. (Color online) The tenfold classification of gapless topological materials depends on the location of the Fermi surfaces in the Brillouin zone, which in turn determines how the Fermi surfaces transform under global antiunitary symmetries (see Table I). (a) Each Fermi surface (red point/line) is left invariant under global (i.e., nonspatial) symmetries. The contour, on which the topological invariant is defined, is indicated by blue circles/spheres. Here, d denotes the spatial dimension and $p = d - d_{\mathrm{FS}}$ is the codimension of the Fermi surface. (b) Different Fermi surfaces are pairwise related to each other by global symmetries ($\mathbf{k} \leftrightarrow -\mathbf{k}$).

1. *Fermi surfaces at high-symmetry points*

As shown in Refs. [26,33–35], Fermi surfaces located at high-symmetry points in the BZ can be protected by

TABLE I. Tenfold classification of topological insulators and fully gapped superconductors [6–9] as well as of Fermi surfaces and nodal point/lines in semimetals and nodal superconductors, respectively [33–35]. The first row indicates the spatial dimension d of topological insulators and superconductors, whereas the second and third rows specify the codimension $p = d - d_{\mathrm{FS}}$ of the Fermi surfaces (nodal lines) at high-symmetry points [Fig. 1(a)] and away from high-symmetry points of the Brillouin zone [Fig. 1(b)], respectively. The first column gives the name of the symmetry classes. The labels T, C, and S in the last three columns indicate the presence ("+," "−," and "1") or absence ("0") of time-reversal, particle-hole, and chiral symmetries, respectively, as well as the sign of the squared symmetry operators T^2 and C^2.

Top. insul. and top. SC	$d=1$	$d=2$	$d=3$	$d=4$	$d=5$	$d=6$	$d=7$	$d=8$			
FS at high-sym. point	$p=8$	$p=1$	$p=2$	$p=3$	$p=4$	$p=5$	$p=6$	$p=7$	T	C	S
FS off high-sym. point	$p=2$	$p=3$	$p=4$	$p=5$	$p=6$	$p=7$	$p=8$	$p=1$			
A	0	$\mathbb{Z}$	0	$\mathbb{Z}$	0	$\mathbb{Z}$	0	$\mathbb{Z}$	0	0	0
AIII	$\mathbb{Z}$	0	$\mathbb{Z}$	0	$\mathbb{Z}$	0	$\mathbb{Z}$	0	0	0	1
AI	0	0	0	$2\mathbb{Z}$	0	$\mathbb{Z}_2$[a,b]	$\mathbb{Z}_2$[a,b]	$\mathbb{Z}$	+	0	0
BDI	$\mathbb{Z}$	0	0	0	$2\mathbb{Z}$	0	$\mathbb{Z}_2$[a,b]	$\mathbb{Z}_2$[a,b]	+	+	1
D	$\mathbb{Z}_2$[a,b]	$\mathbb{Z}$	0	0	0	$2\mathbb{Z}$	0	$\mathbb{Z}_2$[a,b]	0	+	0
DIII	$\mathbb{Z}_2$[a,b]	$\mathbb{Z}_2$[a,b]	$\mathbb{Z}$	0	0	0	$2\mathbb{Z}$	0	−	+	1
AII	0	$\mathbb{Z}_2$[a,b]	$\mathbb{Z}_2$[a,b]	$\mathbb{Z}$	0	0	0	$2\mathbb{Z}$	−	0	0
CII	$2\mathbb{Z}$	0	$\mathbb{Z}_2$[a,b]	$\mathbb{Z}_2$[a,b]	$\mathbb{Z}$	0	0	0	−	−	1
C	0	$2\mathbb{Z}$	0	$\mathbb{Z}_2$[a,b]	$\mathbb{Z}_2$[a,b]	$\mathbb{Z}$	0	0	0	−	0
CI	0	0	$2\mathbb{Z}$	0	$\mathbb{Z}_2$[a,b]	$\mathbb{Z}_2$[a,b]	$\mathbb{Z}$	0	+	−	1

[a] $\mathbb{Z}_2$ numbers only protect Fermi surfaces of dimension zero ($d_{\mathrm{FS}} = 0$) at high-symmetry points of the Brillouin zone.

[b] Fermi surfaces located away from high-symmetry points of the Brillouin zone cannot be protected by a $\mathbb{Z}_2$ topological number. Nevertheless, the system can exhibit gapless surface states (at time-reversal-invariant momenta of the surface Brillouin zone) that are protected by a $\mathbb{Z}_2$ topological invariant.

either $\mathbb{Z}$-type or $\mathbb{Z}_2$-type invariants. The complete tenfold classification of Fermi surfaces that are left invariant under global symmetries is shown in Table I, where the second row indicates the codimension p of the Fermi surface at a high-symmetry point. This result has been obtained using a dimensional reduction procedure [33] and an approach based on K theory [26,34,35]. In Appendix A, we present yet another derivation of this classification scheme by considering all possible symmetry-allowed mass terms that can be added to a representative Dirac-matrix Hamiltonian in a given symmetry class. It is important to note that for a given symmetry class and codimension p, a $\mathbb{Z}$-type topological invariant guarantees the stability of the Fermi surface independent of the Fermi-surface dimension d_{FS}. A $\mathbb{Z}_2$-type topological number, on the other hand, only protects Fermi surfaces of dimension zero, i.e., Fermi points. We can see from Table I that the tenfold classification of global-symmetry-invariant Fermi points (i.e., $d_{\mathrm{FS}} = 0$) is related to the original tenfold classification of topological insulators and superconductors by a dimensional shift, i.e., $d \to d - 1$. Due to a bulk-boundary correspondence [26,33,34], gapless materials with nontrivial topology support protected surface states, which, depending on the case, are either Dirac or Majorana states or are dispersionless, forming flat bands or arc surface states.

Let us illustrate some of the gapless topological states listed in Table I by considering specific lattice models.

a. Nodal superconductor with TRS (class DIII). To demonstrate that $\mathbb{Z}$-type invariants protect Fermi surfaces (nodal lines) of arbitrary dimension d_{FS}, we study the following two-dimensional tight-binding Hamiltonian on the square lattice:

$$H_{\mathrm{s}}^{\mathrm{DIII}} = \sin k_x \sigma_x + \sin k_y \sigma_y, \tag{4}$$

which describes a nodal superconductor with point nodes ($d_{\mathrm{FS}} = 0$) at the four time-reversal-invariant momenta $(0,0)$, $(0,\pi)$, $(\pi,0)$, and (π,π). Hamiltonian (4) preserves time-reversal symmetry, with $T = \sigma_y \mathcal{K}$, and particle-hole symmetry, with $C = \sigma_x \mathcal{K}$. Here, $\mathcal{K}$ denotes the complex-conjugation operator. Since $T^2 = -\mathbb{1}$ and $C^2 = +\mathbb{1}$, the Hamiltonian belongs to symmetry class DIII, where $\mathbb{1}$ is the 2×2 identity matrix. According to Table I, superconducting nodes with codimension $p = 2$ in class DIII are protected by a $\mathbb{Z}$-type topological invariant. Indeed, we find that the winding number

$$\nu = \frac{i}{2\pi} \int_{\mathcal{C}} q^* dq, \tag{5}$$

where $q = (\sin k_x - i \sin k_y)/\sqrt{\sin^2 k_x + \sin^2 k_y}$ is quantized to ± 1 for closed contours $\mathcal{C}$ encircling one of the four nodal points. Specifically, for an anticlockwise-oriented contour we obtain $\nu = +1$ for the nodes at $(0,0)$ and (π,π), whereas $\nu = -1$ for the nodes at $(0,\pi)$ and $(\pi,0)$. The topological nature of these point nodes results in the appearance of protected flat-band edge states for all edge orientations, except the (10) and (01) faces. As demonstrated in Fig. 2(a), these flat-band states connect two projected nodal points with different topological charge (i.e., different winding number ν) in the edge BZ. The BdG Hamiltonian (4) can be converted in a straightforward manner to a three-dimensional topological superconductor with protected line nodes ($d_{\mathrm{FS}} = 1$) by including an extra momentum-space coordinate. Similar to the two-dimensional example [Eq. (4)], the stability of these nodal lines is guaranteed by the quantized winding number ν [Eq. (5)].

b. Semimetal with TRS (class AII). As stated above, $\mathbb{Z}_2$-type invariants only protect Fermi surfaces of dimension zero ($d_{\mathrm{FS}} = 0$) at high-symmetry points of the BZ and cannot give rise to topologically stable Fermi surfaces with $d_{\mathrm{FS}} > 0$. To exemplify this, we consider the following two-dimensional Bloch Hamiltonian on the square lattice:

$$H_{\mathrm{s}}^{\mathrm{AII}} = \sin k_x \sigma_x + \sin k_y \sigma_y + \sin(k_x + k_y)\sigma_z \tag{6}$$

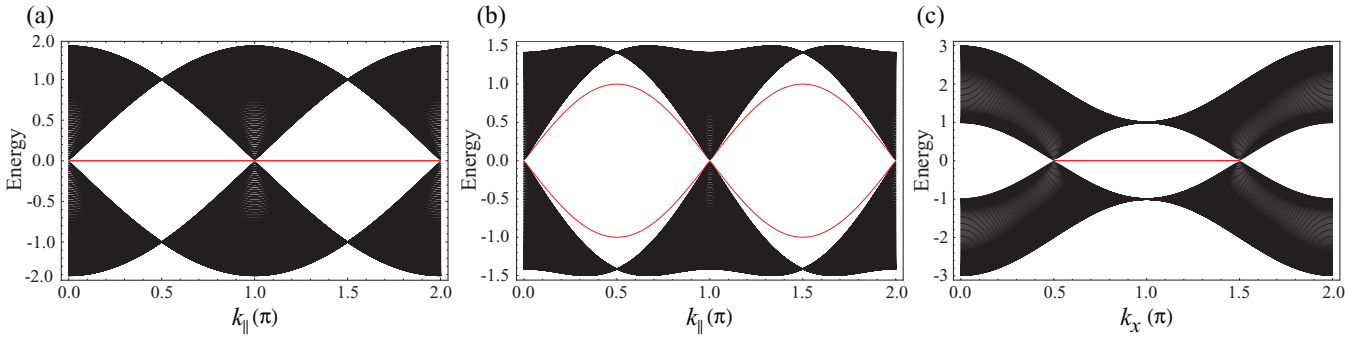

FIG. 2. (Color online) (a) Edge band structure of the nodal topological superconductor (4) (class DIII) for the (11) face as a function of edge momentum $k_\parallel = (k_x + k_y)/\sqrt{2}$. The flat-band edge states (red traces) are protected by time-reversal symmetry and particle-hole symmetry. (b) Band structure of the time-reversal-invariant semimetal (A9) (class AII) at the (11) edge as a function of edge momentum $k_\parallel$. Linearly dispersing edge states (red traces) connect the projected Fermi points in the edge BZ. (c) Edge spectrum of the sublattice-symmetric (chiral-symmetric) semimetal (14) with $A = B = 0.7$ at the (01) face as a function of edge momentum k_x. The flat-band edge states (red trace) are protected by sublattice (chiral) symmetry.

that describes a semimetal with Fermi points at the four time-reversal-invariant momenta of the two-dimensional BZ. Hamiltonian (A9) preserves time-reversal symmetry, with $T = \sigma_y\mathcal{K}$, but breaks particle-hole symmetry, thus belonging to symmetry class AII. The four Fermi points are protected by a binary $\mathbb{Z}_2$ invariant, which can be defined in terms of an extension of H_s^{AII} to three dimensions [34,68]:

$$\widetilde{H}_s^{\mathrm{AII}}(k,\theta) = [\sin k_x\sigma_x + \sin k_y\sigma_y + \sin(k_x + k_y)\sigma_z]\sin\theta + \sigma_z\cos\theta, \quad (7)$$

where $\theta \in [0,\pi]$ is the parameter for the extension in the third direction. The extended Hamiltonian (7) is required to preserve TRS:

$$T^{-1}\widetilde{H}_s^{\mathrm{AII}}(-k,\pi-\theta)T = \widetilde{H}_s^{\mathrm{AII}}(k,\theta). \quad (8)$$

Performing a small-momentum expansion around a given Fermi point, we find that the $\mathbb{Z}_2$ invariant is expressed as

$$n_{\mathbb{Z}_2} = \frac{1}{4\pi}\int_0^{2\pi} d\phi \int_0^{\pi} d\theta\, \hat{\mathbf{g}}\cdot(\partial_\theta\hat{\mathbf{g}}\times\partial_\phi\hat{\mathbf{g}}) \bmod 2, \quad (9)$$

with $\hat{\mathbf{g}} = \mathbf{g}/|\mathbf{g}|$ and

$$\mathbf{g} = (\pm\tilde{k}_x, \pm\tilde{k}_y, \tilde{k}_x + \tilde{k}_y + \Delta) \quad \text{for } \mathbf{k} = (0,0),(\pi,\pi),$$
$$\mathbf{g} = (\pm\tilde{k}_x, \mp\tilde{k}_y, -\tilde{k}_x - \tilde{k}_y + \Delta) \quad \text{for } \mathbf{k} = (0,\pi),(\pi,0), \quad (10)$$

where $\tilde{k}_x = k\cos\phi\sin\theta$, $\tilde{k}_y = k\sin\phi\sin\theta$, $\Delta = \Delta_0\cos\theta$, and (k, Δ_0) are positive constants. The integral (9) is evaluated along the sphere that surrounds the Fermi point and is required to preserve TRS. We observe that the $\mathbb{Z}_2$ invariant (9) is nontrivial (i.e., $n = 1$) for all four Fermi points, hence indicating the topological protection of these two-dimensional Dirac points. By the bulk-boundary correspondence, the topological characteristics of these Fermi points leads to linearly dispersing edge modes, which connect two projected Dirac points in the edge BZ [see Fig. 2(b)]. Importantly, we find that Hamiltonian (A9) cannot be converted to a three-dimensional semimetal with Fermi lines since it is possible to gap out the Fermi lines located at $(0,0,k_z)$, $(0,\pi,k_z)$, $(\pi,0,k_z)$, and (π,π,k_z) by the symmetry-preserving term $\sin k_z\sigma_z$. That is, in the presence of Fermi *lines* along the k_z direction, the topological invariant (9) is ill defined for $k_z \neq 0,\pi$ since it breaks TRS.

c. Unstable semimetal with TRS and PHS (class BDI). As an example of an unstable semimetal in two dimensions, we consider the square-lattice Hamiltonian

$$H_s^{\mathrm{BDI}} = \sin k_x\,\sigma_x\otimes\sigma_y + \sin k_y\,\sigma_y\otimes\mathbb{1}, \quad (11)$$

which represents a four-band semimetal with Fermi points at the four time-reversal-invariant momenta. Hamiltonian (11) belongs to class BDI since it is both time-reversal and particle-hole symmetric with $T = \mathbb{1}\otimes\mathbb{1}\mathcal{K}$ and $C = \sigma_z\otimes\mathbb{1}\mathcal{K}$, respectively. In agreement with the classification of Table I, the four Fermi points of H_s^{BDI} are unstable, as they can be gapped out by the symmetry-preserving mass $\sigma_x\otimes\sigma_z$. This is in accordance with the fact that the winding number

$$\nu = \frac{i}{2\pi}\int_{\mathcal{C}} \mathrm{Tr}\,(\mathbf{q}^\dagger d\mathbf{q}), \quad (12)$$

where

$$\mathbf{q} = \frac{-i}{\sqrt{\sin^2 k_x + \sin^2 k_y}}\begin{pmatrix}\sin k_y & \sin k_x\\ -\sin k_x & \sin k_y\end{pmatrix} \quad (13)$$

vanishes identically for *any* closed contour $\mathcal{C}$.

2. *Fermi surfaces off high-symmetry points*

Second, we discuss the topological classification of semimetals and nodal superconductors with Fermi surfaces (or superconducting nodes) that are located away from high-symmetry points of the BZ. In this case, global antiunitary symmetries pairwise relate different Fermi surfaces with each other [see Fig. 1(b)]. Interestingly, only $\mathbb{Z}$-type invariants can guarantee the stability of Fermi surfaces off high-symmetry points. $\mathbb{Z}_2$-type numbers, on the other hand, cannot protect these Fermi surfaces, but may nevertheless lead to the appearance of zero-energy surface states at time-reversal-invariant momenta of the surface BZ. The complete classification of Fermi surfaces that are pairwise related by global symmetries is shown in Table I, where the third row indicates the codimension p of the Fermi surface located away from

high-symmetry points (cf. Appendix A). We observe that the classification for the two complex symmetry classes A and AIII is identical to the one of Fermi surfaces that are left invariant by global symmetries, while the classification for the eight real symmetry classes is different. As before, we notice that this classification scheme is related to the original tenfold classification of topological insulators and superconductors by a dimensional shift, i.e., in this case $d \to d+1$.

In order to exemplify some of the gapless topological states with Fermi surfaces away from high-symmetry points, we consider a few specific lattice modes.

a. Two-dimensional semimetal with SLS (class AIII). To demonstrate that $\mathbb{Z}$-type invariants protect Fermi surfaces at non-high-symmetry points of the BZ, we study the following sublattice symmetric Hamiltonian on the square lattice:

$$H_{\rm n}^{\rm AIII} = X\sigma_x + Y\sigma_y, \tag{14}$$

where $X = 1+\cos k_y + A\sin k_x + B\cos k_x$ and $Y = \sin k_y$. Sublattice symmetry acts on $H_{\rm n}^{\rm AIII}$ as $SH_{\rm n}^{\rm AIII} + H_{\rm n}^{\rm AIII}S = 0$, with the unitary matrix $S = \sigma_z$. Hamiltonian (14) exhibits two Fermi points located at (δ,π) and $(\delta-\pi,\pi)$, where $\delta = \arctan(-B/A)$ and we require that $\sqrt{A^2+B^2} < 2$. Note that, in agreement with the fermion-doubling theorem by Nielsen and Ninomiya [69], the number of Fermi points is even. Since there exists no symmetry-allowed mass term that can be added to Hamiltonian (14), the two Fermi points are stable and, according to Table I, protected by the $\mathbb{Z}$ topological number Eq. (5), with $q = (X-Yi)/\sqrt{X^2+Y^2}$ and $\mathcal{C}$ a closed contour. Choosing $\mathcal{C}$ to be parallel to the k_y axis, we find that $\nu = +1$ for $\delta-\pi < k_x < \delta$, and zero otherwise. Due to an index theorem [70], a nonzero value of the winding number (5) implies the existence of flat-band edge states at zero energy. At the (01) edge, the zero-energy flat-band states appear within the interval $k_x \in [\delta-\pi,\delta]$ of the edge BZ [see Fig. 2(c)].

b. Three-dimensional semimetal with TRS and PHS (class BDI). $\mathbb{Z}$-type numbers can protect Fermi surfaces of arbitrary dimension $d_{\rm FS}$. To demonstrate this for the case of Fermi surfaces located away from high-symmetry points, we consider the following three-dimensional tight-binding model on the cubic lattice:

$$H_{\rm n}^{\rm BDI} = (1+\cos k_y+\cos k_x)\sigma_x + \sin k_y\sigma_y, \tag{15}$$

which realizes a topological semimetal with two Fermi lines at $(\pm\pi/2,\pi,k_z)$. Hamiltonian (15) belongs to symmetry class BDI since it satisfies both TRS and PHS with $T = \mathbb{1}\mathcal{K}$ and $C = \sigma_z\mathcal{K}$, respectively. We observe that the two Fermi lines, which are located away from the time-reversal-invariant momenta of the BZ, transform into each other under particle-hole and time-reversal symmetries [cf. Fig. 1(b)]. As indicated in Table I, the Fermi lines are protected by a $\mathbb{Z}$-type topological invariant, which for the tight-binding model (15) takes the form of Eq. (5), with $q = (1+\cos k_y+\cos k_x) - i\sin k_y$. The integration contour in Eq. (5) can be chosen to be any circle enclosing the Fermi line. (The integration contour does not need to be time-reversal or particle-hole symmetric.) Similar to the class AIII model (14), a nonzero value of this winding number leads to zero-energy flat-band surface states that connect the two projected Fermi lines in the surface BZ.

c. Unstable nodal superconductor with TRS (class DIII). As indicated in Table I, $\mathbb{Z}_2$-type topological numbers do not guarantee the topological stability of Fermi surfaces (superconducting nodes) at non-high-symmetry points of the BZ. Nevertheless, $\mathbb{Z}_2$-type invariants, which are defined on time-reversal-symmetric contours, can give rise to protected gapless surface states. To demonstrate this, we consider an example of an unstable nodal superconductor given by the four-band BdG Hamiltonian

$$H_{\rm n}^{\rm DIII} = (1+\cos k_x+\cos k_y)\sigma_x\otimes\sigma_y + \sin k_x\sigma_y\otimes\mathbb{1}. \tag{16}$$

This superconductor belongs to symmetry class DIII, as it preserves both time-reversal and particle-hole symmetries, with $T = \sigma_y\otimes\mathbb{1}\mathcal{K}$ and $C = \sigma_x\otimes\mathbb{1}\mathcal{K}$, respectively. Hamiltonian (16) exhibits two point nodes at $(\pi,\pm\pi/2)$. These two point nodes, which are positioned away from the high-symmetry points of the BZ, are unstable since the symmetry-preserving extra kinetic term $\sin k_x\,\sigma_x\otimes\sigma_x$ opens up a gap in the entire bulk BZ (cf. Table I). This is corroborated by the fact that the winding number ν for model Hamiltonian (16) is identically zero for any closed contour $\mathcal{C}$, which follows from a similar argument as the one given in the example of Eq. (11). In contrast, the one-dimensional $\mathbb{Z}_2$ number [8,71]

$$n_{\mathbb{Z}_2} = \prod_{\mathbf{K}\in\mathcal{C}} \frac{{\rm Pf}[\omega(\mathbf{K})]}{\sqrt{\det[\omega(\mathbf{K})]}} \tag{17}$$

for Hamiltonian (16) can take on nontrivial values, which however does not lead to a protection of the point nodes of the superconductor (cf. Table I and Appendix A). In Eq. (17), the product is over the two time-reversal-invariant momenta $\mathbf{K}$ (high-symmetry points) of the contour $\mathcal{C}$ and $\omega(\mathbf{K})$ denotes the 2×2 sewing matrix

$$\omega_{\hat{a}\hat{b}}(\mathbf{k}) = \langle u_{\hat{a}}^-(-\mathbf{k})|\, T\, u_{\hat{b}}^-(\mathbf{k})\rangle, \tag{18}$$

with $|u_{\hat{a}}^-(\mathbf{k})\rangle$ the negative-energy BdG wave functions of Hamiltonian (16). Even though $\mathbb{Z}_2$ number (17) does not stabilize point nodes in the bulk, it nevertheless leads to protected zero-energy surface states at time-reversal-invariant momenta of the surface BZ. To exemplify this, we consider two time-reversal-invariant contours $\mathcal{C}$ oriented along the k_x axis with k_y held fixed at $k_y = 0$ or $k_y = \pi$. With these contours, the $\mathbb{Z}_2$ number takes on the values $n = +1$ and -1 at $k_y = 0$ and π, respectively, indicating the existence of a zero-energy edge state at $k_y = \pi$ of the (10) edge BZ of the superconductor. We observe that the unstable nodal superconductor (16) can be connected to a fully gapped topological superconductor without removing the zero-energy edge states. That is, the edge states of Hamiltonian (16) are inherited from the fully gapped topological phase [72].

III. CLASSIFICATION OF REFLECTION-SYMMETRY-PROTECTED GAPLESS TOPOLOGICAL MATERIALS

Having discussed the classification of gapless topological materials in terms of global symmetries, we are now ready to classify reflection-symmetric topological semimetals and nodal superconductors. Reflection symmetries lead to an enrichment of the tenfold classification of topological

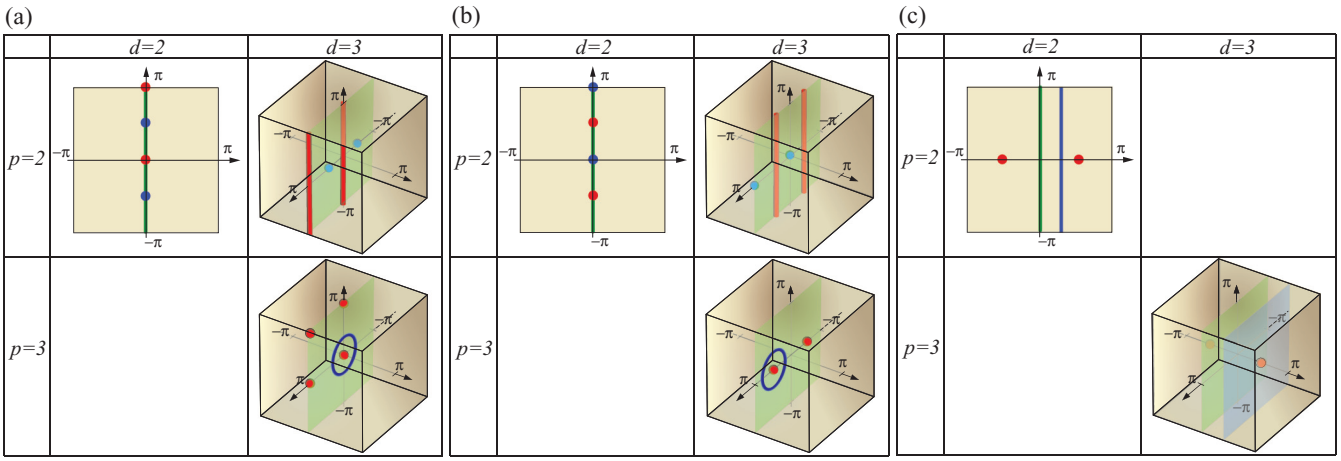

FIG. 3. (Color online) The classification of reflection-symmetry-protected topological semimetals and nodal superconductors depends on the location of the Fermi surfaces with respect to the reflection plane (highlighted in green) in the Brillouin zone, which in turn determines how the Fermi surfaces transform under reflection and global antiunitary symmetries (see Tables II and III). (a) Each Fermi surface (red points/lines) is left invariant under reflection and global antiunitary symmetries. (b) The Fermi surfaces are left invariant by reflection, but transform pairwise into each other by the global antiunitary symmetries. The contours on which the $M\mathbb{Z}$- and $M\mathbb{Z}_2$-type invariants are defined are indicated by blue points/circles in panels (a) and (b). (c) Different Fermi points are pairwise related to each other by both reflection and global symmetries. The contours on which the $C\mathbb{Z}_2$-type invariants are defined are indicated by blue lines/planes (see Table III).

semimetals (nodal superconductors) with new topological phases. The classification depends on the codimension $p = d - d_{\mathrm{FS}}$ of the Fermi surface (nodal line/point) and on whether the reflection operator R commutes or anticommutes with the nonspatial symmetries. Moreover, we need to distinguish how the Fermi surface (nodal line/point) transforms under the mirror reflection and nonspatial symmetries. There are three different cases to be considered: (i) The Fermi surface is invariant under both reflection and global symmetries [Fig. 3(a) and Table II], (ii) Fermi surfaces are invariant under reflection, but transform pairwise into each other by the global antiunitary symmetries [Fig. 3(b) and Table II], and (iii) different Fermi surfaces are pairwise related to each other by both reflection and nonspatial symmetries [Fig. 3(c) and Table III].

Our derivation of these classification schemes, which are presented in Tables II and III, relies primarily on the so-called minimal Dirac-matrix Hamiltonian method [12,73,74]. This method is based on considering reflection-symmetric Dirac-matrix Hamiltonians with the smallest possible matrix dimension for a given symmetry class of the tenfold way. The topological properties of the Fermi surfaces (nodal lines) described by these Dirac-matrix Hamiltonians are then determined by the existence or nonexistence of symmetry-preserving gap-opening terms (SPGTs), i.e., symmetry-allowed terms that fully gap out the bulk Fermi surfaces. The existence of such an SPGT indicates that the Fermi surface is topologically trivial and hence unstable. This is denoted by the label "0" in Tables II and III. On the other hand, if no SPGT exists, then the Fermi surface is topologically stable and protected by a topological invariant (for more details see Appendix A and Ref. [12]). The minimal Dirac-matrix Hamiltonian approach is complemented by a discussion of different types of topological invariants (i.e., $\mathbb{Z}$-, $\mathbb{Z}_2$-, $M\mathbb{Z}$-, $M\mathbb{Z}_2$-, and $C\mathbb{Z}_2$-type invariants) that guarantee the stability of these Fermi surfaces. For some concrete examples, we derive explicit expressions for these topological numbers in Sec. IV. The classification of reflection-symmetric gapless materials in terms of topological invariants is consistent with the Dirac-matrix Hamiltonian method.

Before discussing in detail the classification of reflection-symmetric topological semimetals and nodal superconductors, let us first examine how reflection symmetry acts on the Hamiltonian and how it is related to the global symmetries.

A. Reflection symmetries

Crystal reflection is a spatial symmetry, which acts nonlocally in position space. For concreteness, let us consider a d-dimensional Bloch or BdG Hamiltonian $H(\mathbf{k})$ in momentum space which is invariant under reflection in the first direction. The invariance of $H(\mathbf{k})$ under this mirror symmetry implies

$$R^{-1}H(-k_1,\tilde{\mathbf{k}})R = H(k_1,\tilde{\mathbf{k}}), \tag{19}$$

where $\tilde{\mathbf{k}} = (k_2,\ldots,k_d)$ and the reflection operator R is a unitary matrix. Due to a phase ambiguity in the definition of the reflection operator R [12], we can assume without loss of generality that R is Hermitian (at least for electronic insulators), i.e.,

$$R^\dagger = R. \tag{20}$$

With this assumption, the commutation or anticommutation relations between R and the global nonspatial symmetry operators T, C, and S,

$$SRS^{-1} = \eta_S R,\ TRT^{-1} = \eta_T R,\ CRC^{-1} = \eta_C R, \tag{21}$$

can be determined in an unambiguous way, which in turn simplifies the classification of reflection-symmetry-protected insulators and superconductors. The three indices η_S, η_T, and η_C in Eq. (21) take values $+1$ or -1 and specify whether R commutes $(+1)$ or anticommutes (-1) with the corresponding global symmetry operator. These different possibilities are

TABLE II. Classification of reflection-symmetry-protected topological insulators and fully gapped superconductors [12,13,26], as well as of Fermi surfaces and nodal points/lines in reflection-symmetry-protected semimetals and nodal superconductors, respectively. The first row specifies the spatial dimension d of reflection-symmetry-protected topological insulators and fully gapped superconductors, while the second and third rows indicate the codimension $p = d - d_{\mathrm{FS}}$ of the reflection-symmetric Fermi surfaces (nodal lines) at high-symmetry points [Fig. 3(a)] and away from high-symmetry points of the Brillouin zone [Fig. 3(b)], respectively.

Reflection	Top. insul. and top. SC	$d=1$	$d=2$	$d=3$	$d=4$	$d=5$	$d=6$	$d=7$	$d=8$
	FS within mirror plane at high-sym. point	$p=8$	$p=1$	$p=2$	$p=3$	$p=4$	$p=5$	$p=6$	$p=7$
	FS within mirror plane off high-sym. point	$p=2$	$p=3$	$p=4$	$p=5$	$p=6$	$p=7$	$p=8$	$p=1$
R	A	$M\mathbb{Z}$	0	$M\mathbb{Z}$	0	$M\mathbb{Z}$	0	$M\mathbb{Z}$	0
R_+	AIII	0	$M\mathbb{Z}$	0	$M\mathbb{Z}$	0	$M\mathbb{Z}$	0	$M\mathbb{Z}$
R_-	AIII	$M\mathbb{Z}\oplus\mathbb{Z}$	0	$M\mathbb{Z}\oplus\mathbb{Z}$	0	$M\mathbb{Z}\oplus\mathbb{Z}$	0	$M\mathbb{Z}\oplus\mathbb{Z}$	0
R_+,R_{++}	AI	$M\mathbb{Z}$	0	0	0	$2M\mathbb{Z}$	0	$M\mathbb{Z}_2$[a,b]	$M\mathbb{Z}_2$[a,b]
	BDI	$M\mathbb{Z}_2$[a,b]	$M\mathbb{Z}$	0	0	0	$2M\mathbb{Z}$	0	$M\mathbb{Z}_2$[a,b]
	D	$M\mathbb{Z}_2$[a,b]	$M\mathbb{Z}_2$[a,b]	$M\mathbb{Z}$	0	0	0	$2M\mathbb{Z}$	0
	DIII	0	$M\mathbb{Z}_2$[a,b]	$M\mathbb{Z}_2$[a,b]	$M\mathbb{Z}$	0	0	0	$2M\mathbb{Z}$
	AII	$2M\mathbb{Z}$	0	$M\mathbb{Z}_2$[a,b]	$M\mathbb{Z}_2$[a,b]	$M\mathbb{Z}$	0	0	0
	CII	0	$2M\mathbb{Z}$	0	$M\mathbb{Z}_2$[a,b]	$M\mathbb{Z}_2$[a,b]	$M\mathbb{Z}$	0	0
	C	0	0	$2M\mathbb{Z}$	0	$M\mathbb{Z}_2$[a,b]	$M\mathbb{Z}_2$[a,b]	$M\mathbb{Z}$	0
	CI	0	0	0	$2M\mathbb{Z}$	0	$M\mathbb{Z}_2$[a,b]	$M\mathbb{Z}_2$[a,b]	$M\mathbb{Z}$
R_-,R_{--}	AI	0	0	$2M\mathbb{Z}$	0	$T\mathbb{Z}_2$[a,b,c]	$\mathbb{Z}_2$[a,b]	$M\mathbb{Z}$	0
	BDI	0	0	0	$2M\mathbb{Z}$	0	$T\mathbb{Z}_2$[a,b,c]	$\mathbb{Z}_2$[a,b]	$M\mathbb{Z}$
	D	$M\mathbb{Z}$	0	0	0	$2M\mathbb{Z}$	0	$T\mathbb{Z}_2$[a,b,c]	$\mathbb{Z}_2$[a,b]
	DIII	$\mathbb{Z}_2$[a,b]	$M\mathbb{Z}$	0	0	0	$2M\mathbb{Z}$	0	$T\mathbb{Z}_2$[a,b,c]
	AII	$T\mathbb{Z}_2$[a,b,c]	$\mathbb{Z}_2$[a,b]	$M\mathbb{Z}$	0	0	0	$2M\mathbb{Z}$	0
	CII	0	$T\mathbb{Z}_2$[a,b,c]	$\mathbb{Z}_2$[a,b]	$M\mathbb{Z}$	0	0	0	$2M\mathbb{Z}$
	C	$2M\mathbb{Z}$	0	$T\mathbb{Z}_2$[a,b,c]	$\mathbb{Z}_2$[a,b]	$M\mathbb{Z}$	0	0	0
	CI	0	$2M\mathbb{Z}$	0	$T\mathbb{Z}_2$[a,b,c]	$\mathbb{Z}_2$[a,b]	$M\mathbb{Z}$	0	0
R_{-+}	BDI, CII	$2\mathbb{Z}$	0	$2M\mathbb{Z}$	0	$2\mathbb{Z}$	0	$2M\mathbb{Z}$	0
R_{+-}	DIII, CI	$2M\mathbb{Z}$	0	$2\mathbb{Z}$	0	$2M\mathbb{Z}$	0	$2\mathbb{Z}$	0
R_{+-}	BDI	$M\mathbb{Z}\oplus\mathbb{Z}$	0	0	0	$2M\mathbb{Z}\oplus2\mathbb{Z}$	0	$M\mathbb{Z}_2\oplus\mathbb{Z}_2$[a,b]	$M\mathbb{Z}_2\oplus\mathbb{Z}_2$[a,b]
R_{-+}	DIII	$M\mathbb{Z}_2\oplus\mathbb{Z}_2$[a,b]	$M\mathbb{Z}_2\oplus\mathbb{Z}_2$[a,b]	$M\mathbb{Z}\oplus\mathbb{Z}$	0	0	0	$2M\mathbb{Z}\oplus2\mathbb{Z}$	0
R_{+-}	CII	$2M\mathbb{Z}\oplus2\mathbb{Z}$	0	$M\mathbb{Z}_2\oplus\mathbb{Z}_2$[a,b]	$M\mathbb{Z}_2\oplus\mathbb{Z}_2$[a,b]	$M\mathbb{Z}\oplus\mathbb{Z}$	0	0	0
R_{-+}	CI	0	0	$2M\mathbb{Z}\oplus2\mathbb{Z}$	0	$M\mathbb{Z}_2\oplus\mathbb{Z}_2$[a,b]	$M\mathbb{Z}_2\oplus\mathbb{Z}_2$[a,b]	$M\mathbb{Z}\oplus\mathbb{Z}$	0

[a] $\mathbb{Z}_2$ and $M\mathbb{Z}_2$ invariants only protect Fermi surfaces of dimension zero ($d_{\mathrm{FS}} = 0$) at high-symmetry points of the Brillouin zone.
[b] Fermi surfaces located within the mirror plane but away from high-symmetry points cannot be protected by a $\mathbb{Z}_2$ or $M\mathbb{Z}_2$ topological invariant. Nevertheless, the system can exhibit gapless surface states that are protected by a $\mathbb{Z}_2$ or $M\mathbb{Z}_2$ topological invariant.
[c] For gapless topological materials, the presence of translation symmetry is always assumed. Hence, there is no distinction between $T\mathbb{Z}_2$ and $\mathbb{Z}_2$ for gapless topological materials.

labeled by R_{η_T}, R_{η_S}, and R_{η_C} for the five symmetry classes AI, AII, AIII, C, and D, respectively, which contain only one global symmetry operation. For the remaining four symmetry classes BDI, CI, CII, and DIII, which contain two nonspatial symmetries, the four different possible (anti)commutation relations are denoted by $R_{\eta_T\eta_C}$. Hence, there are a total of 27 different symmetry classes for reflection-symmetry-protected topological insulators and fully gapped superconductors (see Table II). We observe that since the reflection operator R is both Hermitian and unitary, $R^2 = \mathbb{1}$ and all eigenvalues of R are either $+1$ or -1. Here, $\mathbb{1}$ denotes the identity matrix with unspecified matrix dimension.

B. Fermi surfaces at high-symmetry points within mirror planes

Fermi points that are invariant under both reflection and global symmetries [red points in Fig. 3(a)], can be protected by $\mathbb{Z}$-, $M\mathbb{Z}$-, $\mathbb{Z}_2$-, or $M\mathbb{Z}_2$-type topological numbers. The topological classification of these Fermi points ($d_{\mathrm{FS}} = 0$) in d dimensions is related to the classification of reflection-symmetric fully gapped systems in $d+1$ dimensions [12,13,26]. (For a brief review of the classification of fully gapped reflection-symmetric topological materials, see Appendix B.) To demonstrate this relation, let us consider a d-dimensional Dirac Hamiltonian of a reflection-symmetric insulator (or fully gapped superconductor) in a given symmetry class

$$H^{\mathrm{TI}}_{\mathrm{Dirac}} = \sum_{i=1}^{d} k_i \gamma_i + m\tilde{\gamma}_0. \tag{22}$$

Reflection symmetry R is implemented by $R^{-1} H^{\mathrm{TI}}_{\mathrm{Dirac}}(-k_1,\tilde{\mathbf{k}})R = H^{\mathrm{TI}}_{\mathrm{Dirac}}(k_1,\tilde{\mathbf{k}})$. Here and in the following, γ_i denote Dirac matrices which anticommute

TABLE III. Classification of Fermi points and superconducting point nodes of reflection-symmetric semimetals and nodal superconductors, respectively, where the Fermi points (point nodes) are located outside the mirror plane [see Fig. 3(c)]. The first row indicates the spatial dimension d of the semimetal (nodal superconductor). The prefix "C" indicates that the corresponding topological invariant is defined in terms of the combined symmetries $\tilde{T}$ and/or $\tilde{C}$ [see Eq. (26)] on a $(d-1)$-dimensional plane which is perpendicular to the k_1 axis [blue line/plane in Fig. 3(c)]. The $\mathbb{Z}$- and $\mathbb{Z}_2$-type invariants, on the other hand, are identical to the ones of the original tenfold classification in the absence of mirror symmetry (cf. Table I) and are defined on $(d-1)$-dimensional hyperspheres surrounding the Fermi point.

Reflection	FS off mirror plane and off high-sym. point	$d=1$	$d=2$	$d=3$	$d=4$	$d=5$	$d=6$	$d=7$	$d=8$
R	A	$\mathbb{Z}$	0	$\mathbb{Z}$	0	$\mathbb{Z}$	0	$\mathbb{Z}$	0
R_+	AIII	0	$\mathbb{Z}$	0	$\mathbb{Z}$	0	$\mathbb{Z}$	0	$\mathbb{Z}$
R_+, R_{++}	AI	$\mathbb{Z}$	0	0	0	$2\mathbb{Z}$	0	$C\mathbb{Z}_2$	$C\mathbb{Z}_2$
	BDI	$C\mathbb{Z}_2$	$\mathbb{Z}$	0	0	0	$2\mathbb{Z}$	0	$C\mathbb{Z}_2$
	D	$C\mathbb{Z}_2$	$C\mathbb{Z}_2$	$\mathbb{Z}$	0	0	0	$2\mathbb{Z}$	0
	DIII	0	$C\mathbb{Z}_2$	$C\mathbb{Z}_2$	$\mathbb{Z}$	0	0	0	$2\mathbb{Z}$
	AII	$2\mathbb{Z}$	0	$C\mathbb{Z}_2$	$C\mathbb{Z}_2$	$\mathbb{Z}$	0	0	0
	CII	0	$2\mathbb{Z}$	0	$C\mathbb{Z}_2$	$C\mathbb{Z}_2$	$\mathbb{Z}$	0	0
	C	0	0	$2\mathbb{Z}$	0	$C\mathbb{Z}_2$	$C\mathbb{Z}_2$	$\mathbb{Z}$	0
	CI	0	0	0	$2\mathbb{Z}$	0	$C\mathbb{Z}_2$	$C\mathbb{Z}_2$	$\mathbb{Z}$
R_-, R_{--}	AI	$2\mathbb{Z}$	0	$C\mathbb{Z}_2$	0	$2\mathbb{Z}$	0	0	0
	BDI	0	$2\mathbb{Z}$	0	$C\mathbb{Z}_2$	0	$2\mathbb{Z}$	0	0
	D	0	0	$2\mathbb{Z}$	0	$C\mathbb{Z}_2$	0	$2\mathbb{Z}$	0
	DIII	0	0	0	$2\mathbb{Z}$	0	$C\mathbb{Z}_2$	0	$2\mathbb{Z}$
	AII	$2\mathbb{Z}$	0	0	0	$2\mathbb{Z}$	0	$C\mathbb{Z}_2$	0
	CII	0	$2\mathbb{Z}$	0	0	0	$2\mathbb{Z}$	0	$C\mathbb{Z}_2$
	C	$C\mathbb{Z}_2$	0	$2\mathbb{Z}$	0	0	0	$2\mathbb{Z}$	0
	CI	0	$C\mathbb{Z}_2$	0	$2\mathbb{Z}$	0	0	0	$2\mathbb{Z}$
R_{+-}	CI	$C\mathbb{Z}_2$	0	0	0	0	0	0	$C\mathbb{Z}_2$
R_{-+}	BDI	0	$C\mathbb{Z}_2$	$C\mathbb{Z}_2$	0	0	0	0	0
R_{+-}	DIII	0	0	0	$C\mathbb{Z}_2$	$C\mathbb{Z}_2$	0	0	0
R_{-+}	CII	0	0	0	0	0	$C\mathbb{Z}_2$	$C\mathbb{Z}_2$	0
R_-	AIII	0	0	0	0	0	0	0	0
R_{-+}	DIII, CI	0	0	0	0	0	0	0	0
R_{+-}	BDI, CII	0	0	0	0	0	0	0	0

(commute) with the time-reversal operator T (particle-hole operator C) of the given symmetry class, whereas $\tilde{\gamma}_i$ are Dirac matrices that commute (anticommute) with T (C) (see Appendix A). By considering the reflection-symmetric surface states of $H^{\mathrm{TI}}_{\mathrm{Dirac}}$, we can derive from Eq. (22) a Dirac Hamiltonian describing a reflection-symmetric Fermi point in the same symmetry class as Eq. (22) but in one dimension lower,

$$H^R_{\mathrm{s}} = \sum_{i=1}^{d-1} k_i \mathbf{P}\gamma_i \mathbf{P}, \tag{23}$$

with the projection operator $\mathbf{P} = (\mathbb{1} - i\tilde{\gamma}_0\gamma_d)/2$. The topological property of $H^{\mathrm{TI}}_{\mathrm{Dirac}}$ is signaled by the existence or nonexistence of an *extra* symmetry-allowed mass term $\tilde{\Gamma}$ [12], i.e., a symmetry-preserving Dirac matrix that anticommutes with all Dirac matrices γ_i and $\tilde{\gamma}_0$ of Eq. (22). Whenever such an extra mass term $\tilde{\Gamma}$ exists, it is possible to construct an SPGT for H^R_{s} [Eq. (23)] by $\tilde{\Gamma}_{\mathbf{P}} = \mathbf{P}\tilde{\Gamma}\mathbf{P}$, which is nonzero since $\tilde{\Gamma}$ anticommutes with both $\tilde{\gamma}_0$ and γ_d. Vice versa, one can show that whenever there exists an SPGT for H^R_{s}, i.e., a symmetry-allowed Dirac matrix $\tilde{\gamma}$ that anticommutes with H^R_{s}, there is a corresponding extra symmetry-allowed mass term for $H^{\mathrm{TI}}_{\mathrm{Dirac}}$ [12,66]. Hence, the classification of Fermi points (i.e., $d_{\mathrm{FS}} = 0$) at high-symmetry positions within the mirror plane follows from the classification of reflection-symmetric fully gapped systems by the dimensional shift $d \to d-1$ (Table II). We observe that this finding is in agreement with the classification of Fermi points reported by Shiozaki and Sato in Ref. [26] [see Eq. (9.5) in their work].

For Fermi surfaces with $d_{\mathrm{FS}} > 0$, on the other hand, the classification differs from the one of Fermi points ($d_{\mathrm{FS}} = 0$). That is, only $\mathbb{Z}$-type invariants (i.e., $\mathbb{Z}$, $M\mathbb{Z}$, and $M\mathbb{Z} \oplus \mathbb{Z}$ topological numbers) can protect Fermi surfaces with $d_{\mathrm{FS}} > 0$. This is because for a gapless d-dimensional system with, e.g., Fermi lines along the k_d direction [described by Eq. (23)], we can add to the Hamiltonian the additional symmetry-preserving kinetic term $k_d\gamma_d$, which gaps out the Fermi lines (except at high-symmetry points). For gapless systems with a $\mathbb{Z}_2$-type invariant, such an extra kinetic term always exists, whereas for Fermi surfaces with a $\mathbb{Z}$-type topological number this extra kinetic term is absent (cf. Appendix A for more details and Sec. IV A for some examples).

The classification of Fermi surfaces that are located within the mirror plane at high-symmetry positions is summarized in Table II, where the second row indicates the codimension p of the Fermi surface. The prefix "M" in Table II indicates that the corresponding topological invariant is defined on

a $(p-2)$-dimensional contour within the reflection plane [blue points/lines in Fig. 3(a)]. The topological invariants labeled by $\mathbb{Z}$ and $\mathbb{Z}_2$, on the other hand, are defined on $(p-1)$-dimensional contours that intersect with the mirror plane (same invariants as in the absence of reflection symmetry, cf. Table I).

C. Fermi surfaces within mirror planes but off high-symmetry points

Second, we classify Fermi surfaces that are located within the mirror plane but away from high-symmetry points [Fig. 3(b)]. These Fermi surfaces are invariant under reflection, but transform pairwise into each other by the nonspatial antiunitary symmetries. We discuss this classification by considering the following reflection-symmetric Dirac-matrix Hamiltonian

$$H_n^R = \sum_{i=1}^{p-1} \sin k_i \gamma_i + \left(1 - p + \sum_{i=1}^{p} \cos k_i\right) \tilde{\gamma}_0, \tag{24}$$

which describes a semimetal (nodal superconductor) with a $(d-p)$-dimensional Fermi surface (superconducting node) located at

$$\mathbf{k} = (0, \ldots, 0, \pm \pi/2, k_{p+1}, \ldots, k_d). \tag{25}$$

Reflection symmetry acts on Hamiltonian (24) as $R^{-1} H_n^R(-k_1, \tilde{\mathbf{k}}) R = H_n^R(k_1, \tilde{\mathbf{k}})$. We observe that Fermi surface (25) lies within the mirror plane $k_1 = 0$, but away from the high-symmetry points $(0,0,0,\ldots,0)$, $(\pi,0,0,\ldots,0)$, $(0,\pi,0,\ldots,0)$, etc., of the BZ. Comparing Eq. (24) to (22) we find that H_n^R, with $k_p \neq \pm\pi/2$ and $k_{p-1}, \ldots, k_d$ held fixed, can be interpreted as a reflection-symmetric insulator (fully gapped superconductor) in $d = p-1$ dimensions. Hence, the existence (or nonexistence) of an extra symmetry-allowed mass term $\tilde{\Gamma}$ for $H_{\text{Dirac}}^{\text{TI}}$ [Eq. (22)] implies the existence (or nonexistence) of a *momentum-independent* SPGT for H_n^R [Eq. (24)]. However, Fermi surface (25) can also be gapped out by an additional symmetry-allowed kinetic term, i.e., by the momentum-dependent SPGT $\sin k_p \gamma_p$. It turns out that for symmetry classes with a $\mathbb{Z}_2$- or $M\mathbb{Z}_2$-type invariant, this extra kinetic term is always allowed by symmetry, whereas for classes with a $\mathbb{Z}$- or $M\mathbb{Z}$-type number, this term is symmetry forbidden (cf. Appendix A). With this, it follows that the classification of p-dimensional Fermi surfaces (superconducting nodes) within the reflection plane but off high-symmetry points is given by the classification of reflection-symmetric topological insulators (fully gapped superconductors) in $d = p-1$ dimensions which are protected by a $\mathbb{Z}$- or $M\mathbb{Z}$-type invariant (cf. Table II). We note that while $\mathbb{Z}_2$- or $M\mathbb{Z}_2$-type invariants cannot protect Fermi surfaces that are located within the mirror plane but away from high-symmetry points, they nevertheless might give rise to protected gapless surface states (see Sec. IV B 4 for an example).

D. Fermi surfaces outside mirror planes

Finally, we discuss the classification of Fermi surfaces (superconducting nodes) that are located outside the mirror plane. These Fermi surfaces are pairwise related to each other by both reflection and nonspatial antiunitary symmetries [see Fig. 3(c)]. Reflection symmetry alone cannot protect Fermi surfaces that lie outside the reflection plane since the reflection symmetry does not restrict the form of the mass term at the position of the Fermi surface. However, a combination of reflection and global antiunitary symmetries can give rise to topologically stable Fermi points (or point nodes in the superconducting gap) [8,75]. In order to study this possibility, we introduce the combined symmetry operators

$$\tilde{T} = RT \quad \text{and} \quad \tilde{C} = RC, \tag{26a}$$

which are antiunitary. These combined symmetry operators act on the d-dimensional Bloch or BdG Hamiltonian as follows:

$$\tilde{T}^{-1} H(k_1, -\tilde{\mathbf{k}}) \tilde{T} = +H(k_1, \tilde{\mathbf{k}}) \tag{26b}$$

and

$$\tilde{C}^{-1} H(k_1, -\tilde{\mathbf{k}}) \tilde{C} = -H(k_1, \tilde{\mathbf{k}}). \tag{26c}$$

Hence, $\tilde{T}$ $(\tilde{C})$ can be viewed as an effective time-reversal (particle-hole) symmetry acting within $(d-1)$-dimensional planes that are perpendicular to the k_1 direction [blue lines/planes in Fig. 3(c)]. For each of these planes, it is possible to define a topological number and study its evolution as a function of the parameter k_1 [62]. These k_1-dependent topological numbers can only change across gap-closing points. Hence, the stability of Fermi points or superconducting point nodes (i.e., gap-closing points) can be discussed in terms of these topological invariants which are defined in the presence of the combined symmetry $\tilde{T}$ and/or $\tilde{C}$ [Eq. (26)]. Moreover, at surfaces that are parallel to the k_1 direction, these k_1-dependent topological numbers give rise to arc surface states that connect two projected Fermi points in the surface BZ.

In this section, we derive the classification of Fermi surfaces outside the mirror plane by examining which types of topological invariants can be defined within the $(d-1)$-dimensional planes perpendicular to the k_1 axis. For this, we have to distinguish between two different kinds of invariants: (i) mirror invariants that are defined within the mirror plane for a given eigenspace of the reflection operator R and (ii) invariants which are defined for any given plane perpendicular to the k_1 axis [green and blue lines/planes in Fig. 3(c), respectively]. Since these two kinds of invariants are constrained differently by symmetry, they can in principle give rise to different classifications. However, it turns out that the Fermi points are only protected by the "weaker" of these two invariants. That is, e.g., if one invariant is of $\mathbb{Z}$ type whereas the other one is of $\mathbb{Z}_2$ type, then the Fermi points only exhibit a $\mathbb{Z}_2$-type topological characteristic. This follows from the fact that the topological invariant cannot change as a function of k_1 as long as the bulk gap does not close. Hence, the invariant defined in the mirror plane must equal the invariant defined in a plane that is perpendicular to k_1 and infinitesimally close to the mirror plane. This condition can only be satisfied if the "stronger" of the two invariants reduces to the "weaker" one. In Appendix C, we present a complementary derivation of the classification scheme of Table III using the Dirac-matrix Hamiltonian approach.

Le us now discuss in detail for which of the 27 symmetry classes listed in Tables II and III there exist topologically

stable Fermi points (point nodes) protected by the combined symmetry $\tilde{T}$ and/or $\tilde{C}$.

1. R_+ and R_{++}

First, we study the situation where the reflection symmetry operator R commutes with all global antiunitary symmetries, which is denoted by R_+ and R_{++} in Table III. Since $[R,T]=0$ and $[R,C]=0$, we have $\tilde{T}^2=T^2$ and $\tilde{C}^2=C^2$, from which it follows that the tenfold symmetry class defined in terms of T and C is the same as the one defined in terms of the combined symmetries $\tilde{T}$ and $\tilde{C}$. Hence, the classification of R_+ (R_{++}) reflection-symmetric systems with Fermi points outside the reflection plane is almost the same as the classification of Fermi points off high-symmetry momenta in the absence of reflection symmetry (compare Table I with Table III and see Appendix C 1). The only difference is that the $C\mathbb{Z}_2$-type invariants of Table III, which are defined in terms of the combined symmetries (26), lead to stable Fermi points outside the reflection plane, whereas the $\mathbb{Z}_2$-type invariants of Table I do not protect Fermi points that are located away from high-symmetry momenta (cf. Sec. II A 2). We observe that for systems with R_+ (R_{++}) reflection symmetry in Table III the mirror invariants which are defined in the mirror planes for a given eigenspace of R yield the same classification as the invariants which are defined in the planes perpendicular to k_1 with $k_1\neq 0,\pi$.

2. R_- and R_{--}

Second, we study the case where the reflection operator R anticommutes with the nonspatial symmetries T and C, which is labeled by R_- and R_{--} in Table III. Here, we find that $\tilde{T}^2=-T^2$ and $\tilde{C}^2=-C^2$ which implies that the symmetry class defined in terms of $\tilde{T}$ and $\tilde{C}$ is shifted by four positions on the "Bott clock" [73] with respect to the symmetry class defined in terms of T and C. Note that since the "Bott clock" has periodicity eight, the direction of the shift is irrelevant. Therefore, the types of invariants that can be defined in $(d-1)$-dimensional planes with fixed $k_1\neq 0,\pi$ can be inferred from column $p=d+4$ of the classification of Fermi surfaces that are away from high-symmetry points (Table I). This, however, is inconsistent with the invariants that can be defined within the mirror planes $k_1=0,\pi$. That is, since $[H(k_1=0,\pi;\tilde{\mathbf{k}}),R]=0$ and $[S=TC,R]=0$, it is possible to block-diagonalize H within the mirror plane with respect to R, and for each block one can define a Chern number (class BDI, DIII, CII, and CI) or a winding number (class AI, D, AII, and C). For example, for three-dimensional systems, there are the following invariants that can be defined within the mirror planes (fixed $k_1=0,\pi$) or within planes with fixed $k_1\neq 0,\pi$:

$d=3$	AI	BDI	D	DIII	AII	CII	C	CI
Mirror plane	$\mathbb{Z}$	0	$\mathbb{Z}$	0	$\mathbb{Z}$	0	$\mathbb{Z}$	0
$(k_1\neq 0,\pi)$ plane	$\mathbb{Z}_2$	0	$\mathbb{Z}$	0	0	0	$\mathbb{Z}$	$\mathbb{Z}_2$

As discussed above, the Fermi points are only protected by the "weaker" of these two invariants [76]. Extending these arguments to other dimensions yields the classification shown in Table III [77]. The derivation of this result using the Dirac-matrix Hamiltonian approach is given in Appendix C 2. We observe that the classification for classes with $\mathbb{Z}$-type invariants almost agrees with the classification of Fermi points located away from high-symmetry momenta in the absence of reflection symmetry (Table I). The only difference is that reflection symmetry requires that the $\mathbb{Z}$ invariants are even (indicated by "$2\mathbb{Z}$" in Table III), whereas in the absence of reflection symmetry the $\mathbb{Z}$ numbers can also take on odd values.

3. DIII and CI with R_{+-} and BDI and CII with R_{-+}

Third, we discuss the case where the reflection operator R commutes with one of the global antiunitary symmetries but anticommutes with the other one, i.e., classes DIII and CI with R_{+-}-type reflection symmetry and classes BDI and CII with R_{-+}-type reflection symmetry. From the (anti-)commutation relations of R with the nonspatial symmetries we find that the symmetry class defined in terms of $\tilde{T}$ and $\tilde{C}$ (symmetry class for plane with fixed $k_1\neq 0,\pi$) is shifted with respect to the symmetry class defined in terms of T and C (symmetry class of entire system) as follows:

$$\text{DIII}\to\text{CII},\ \text{CII}\to\text{CI},\ \text{CI}\to\text{BDI},\ \text{BDI}\to\text{DIII}. \tag{27a}$$

On the other hand, since only one global symmetry commutes with the reflection operator R, the symmetry class within the mirror plane is reduced in the following way:

$$\text{DIII}\to\text{AII},\ \text{CI}\to\text{AI},\ \text{BDI}\to\text{D},\ \text{CII}\to\text{C}. \tag{27b}$$

By a similar logic as above, we find by use of Eq. (27) and Table I that, e.g., for three-dimensional systems, the following invariants can be defined within the mirror planes (fixed $k_1=0,\pi$) or within planes with fixed $k_1\neq 0,\pi$:

$d=3$	DIII	CI	BDI	CII
Mirror plane	$\mathbb{Z}_2$	0	$\mathbb{Z}$	$\mathbb{Z}$
$(k_1\neq 0,\pi)$ plane	0	0	$\mathbb{Z}_2$	0

As before, we find that only the "weaker" of these two types of invariants leads to a protection of the Fermi point (cf. Appendix C 4). Extending these arguments to other dimensions gives the classification of Table III.

4. AIII with R_-, DIII and CI with R_{-+}, and BDI and CII with R_{+-}

Finally, we consider class AIII with R_--type reflection symmetry, classes DIII and CI with R_{-+}-type reflection symmetry, and classes BDI and CII with R_{+-}-type reflection symmetry. Repeating the steps of the previous subsection, we find that for, e.g., three-dimensional systems, the following invariants can be defined within the mirror plane and within

planes with fixed $k_1 \neq 0,\pi$:

$d=3$	AIII	DIII	CI	BDI	CII
Mirror plane	$\mathbb{Z}$	$\mathbb{Z}$	0	$2\mathbb{Z}$	$\mathbb{Z}_2$
$(k_1 \neq 0,\pi)$ plane	0	0	0	0	$\mathbb{Z}_2$

,

which suggests that Fermi points in three-dimensional systems with class CII symmetries are protected by a $\mathbb{Z}_2$-type invariant. However, this is in contradiction with the result obtained from the Dirac-matrix Hamiltonian approach, which shows that all Fermi points have trivial topology (Appendix C 3). It turns out that even though some nontrivial $\mathbb{Z}_2$-type invariants can in principle be defined, these invariants do not protect Fermi points outside the mirror plane. We conclude that Fermi points outside the mirror plane in class AIII with R_--type reflection symmetry, classes DIII and CI with R_{-+}-type reflection symmetry, and classes BDI and CII with R_{+-}-type reflection symmetry have trivial topology in all spatial dimensions (Table III).

IV. EXAMPLES OF REFLECTION-SYMMETRY-PROTECTED TOPOLOGICAL SEMIMETALS AND NODAL SUPERCONDUCTORS

In this section, we present several examples of gapless topological phases protected by reflection symmetry. As in Sec. III, we consider three different types of Fermi-surface positions, which are defined by how the Fermi surface transforms under the mirror reflection and nonspatial symmetries (see Fig. 3).

A. Fermi surfaces at high-symmetry points within mirror planes

We start by discussing four examples of reflection-symmetry-protected Fermi surfaces (superconducting nodes) that are left invariant under both reflection and global symmetries. These Fermi surfaces are located at high-symmetry points within the reflection plane [see Fig. 3(a)].

1. *Reflection-symmetric nodal spin-triplet superconductor with TRS (class DIII with R_{-+} and $p=2$)*

As indicated in Table II, point nodes ($d_{\mathrm{FS}}=0$) in two-dimensional spin-triplet superconductors with TRS and R_{-+}-type reflection symmetry (class DIII with R_{-+}) are protected by an $M\mathbb{Z}\oplus\mathbb{Z}$ invariant. That is, the number of protected point nodes at high-symmetry points within the mirror plane is given by $\max\{|n_{\mathbb{Z}}|,|n_{M\mathbb{Z}}|\}$, where $n_{\mathbb{Z}}$ denotes the one-dimensional winding number, whereas $n_{M\mathbb{Z}}$ is the mirror invariant. Let us illustrate this type of reflection-symmetric nodal superconductor by considering the following continuum model:

$$H_s^{\mathrm{DIII}} = k_x\sigma_x + k_y\sigma_y. \tag{28}$$

This superconductor has a point node at $\mathbf{k}=(0,0)$ and is invariant under reflection $k_x \to -k_x$ with $R=\sigma_y$. Time-reversal and particle-hole symmetry operators are given by $T=\sigma_y\mathcal{K}$ and $C=\sigma_x\mathcal{K}$, respectively. Since $\{T,R\}=0$ and $[C,R]=0$, Hamiltonian (28) exhibits an R_{-+}-type reflection symmetry. The global invariant $n_{\mathbb{Z}}$ of this nodal superconductor is given by the one-dimensional winding number [Eq. (5)] with $q=(k_x-ik_y)/\sqrt{k_x^2+k_y^2}$ and an integration contour $\mathcal{C}$ that surrounds the point node at $\mathbf{k}=(0,0)$. We find that this winding number evaluates to $n_{\mathbb{Z}}=+1$. The mirror number $n_{M\mathbb{Z}}$, on the other hand, is defined on the mirror line $k_x=0$ for each eigenspace of the mirror operator R (i.e., $\sigma_y=\pm1$). For Eq. (28), the mirror number is given by the difference of occupied states on either side of the point node

$$n_{M\mathbb{Z}}^{\pm} = n_{\mathrm{occ}}^{\pm}(k_y>0) - n_{\mathrm{occ}}^{\pm}(k_y<0) = \mp 1, \tag{29}$$

where $n_{\mathrm{occ}}^{\pm}(k_y)$ denotes the number of occupied states (i.e., the number of negative-energy states) at $\mathbf{k}=(0,k_y)$ in the eigenspace of R with eignevalue ±1. Hence, the nodal point at $\mathbf{k}=(0,0)$ is protected by both the winding number $n_{\mathbb{Z}}$ and the mirror number $n_{M\mathbb{Z}}^{\pm}$.

It is important to note, however, that gapless systems with $M\mathbb{Z}\oplus\mathbb{Z}$-type invariants are *not* protected by the sum of the $\mathbb{Z}$ and $M\mathbb{Z}$ invariants; rather, the number of point nodes (gapless modes) is given by $\max\{|n_{\mathbb{Z}}|,|n_{M\mathbb{Z}}|\}$. To exemplify this further, we consider two doubled versions of Hamiltonian (28):

$$H_{s,1}^{\mathrm{DIII}} = k_x\sigma_x\otimes\sigma_z + k_y\sigma_y\otimes\sigma_z \tag{30a}$$

and

$$H_{s,2}^{\mathrm{DIII}} = k_x\sigma_x\otimes\sigma_z + k_y\sigma_y\otimes\mathbb{1}, \tag{30b}$$

which have the same symmetry properties as Eq. (28) with $T=\sigma_y\otimes\mathbb{1}\mathcal{K}$, $C=\sigma_x\otimes\mathbb{1}\mathcal{K}$, and $R=\sigma_y\otimes\mathbb{1}$. Equations (30a) and (30b) have different topological characteristics: While the topology of $H_{s,1}^{\mathrm{DIII}}$ is given by $n_{\mathbb{Z}}=2$ and $n_{M\mathbb{Z}}^{\pm}=0$, for $H_{s,2}^{\mathrm{DIII}}$ we find that $n_{\mathbb{Z}}=0$ and $n_{M\mathbb{Z}}^{\pm}=\mp2$. Hence, both Hamiltonians in Eq. (30) exhibit two stable gapless modes at $\mathbf{k}=0$. We now form a direct product between $H_{s,1}^{\mathrm{DIII}}$ and $H_{s,2}^{\mathrm{DIII}}$, which yields an 8×8 Hamiltonian $H_{s,3}^{\mathrm{DIII}}=\mathrm{diag}(H_{s,1}^{\mathrm{DIII}},H_{s,2}^{\mathrm{DIII}})$, with four gapless modes. However, only two of these four modes are topologically stable since it is possible to gap out two states by the symmetry-preserving mass term

$$\begin{pmatrix} 0 & 0 & 0 & 0 \\ 0 & 0 & 0 & im\sigma_y \\ 0 & 0 & 0 & 0 \\ 0 & -im\sigma_y & 0 & 0 \end{pmatrix}. \tag{31}$$

Thus, in accordance with the formula $\max\{|n_{\mathbb{Z}}|,|n_{M\mathbb{Z}}|\}=2$, $H_{s,3}^{\mathrm{DIII}}$ exhibits only two stable gapless modes at $\mathbf{k}=0$.

In closing, we observe that by including an extra momentum-space coordinate, we can convert Hamiltonian (28) to a three-dimensional reflection-symmetric superconductor with a protected line node ($d_{\mathrm{FS}}=1$) located at $\mathbf{k}=(0,0,k_z)$. The stability of this nodal line is guaranteed by the quantized winding number $n_{\mathbb{Z}}$ [Eq. (5)] and the mirror invariant $n_{M\mathbb{Z}}$ [Eq. (29)].

2. *Reflection-symmetric Dirac semimetal with TRS (class AII with R_+ and $p=3$)*

Next, we study a reflection-symmetric three-dimensional Dirac semimetal with TRS, which is described by

$$H_s^{\mathrm{AII}} = k_x\sigma_x\otimes\sigma_z + k_y\sigma_y\otimes\mathbb{1} + k_z\sigma_z\otimes\mathbb{1}. \tag{32}$$

Time-reversal and reflection-symmetry operators are given by $T=\sigma_y\otimes\mathbb{1}\mathcal{K}$ and $R=\mathbb{1}\otimes\sigma_x$, respectively. Because $T^2=-\mathbb{1}$ and $[T,R]=0$, Hamiltonian (32) belongs to symmetry

class AII with R_+. The semimetal of Eq. (32) has a Dirac point at $\mathbf{k}=(0,0,0)$ which is topologically stable since there exists no SPGT that can be added to the Hamiltonian. Indeed, according to Table II, this Fermi point is protected by an $M\mathbb{Z}_2$-type topological invariant, which is defined on the mirror line $k_x=0$ for each eigenspace of the reflection operator R. Focusing on the eigenspace $R=+1$, we find that H_s^{AII} in this subspace on the mirror line is given by

$$h_{R=+1}^{\mathrm{AII}} = k_y\sigma_y + k_z\sigma_z. \tag{33}$$

The $M\mathbb{Z}_2$ invariant is defined in terms of an extension of Eq. (33) to three dimensions [cf. Eq. (7)]

$$\widetilde{h}_{R=+1}^{\mathrm{AII}} = (k_y\sigma_y + k_z\sigma_z)\cos\theta + \Delta\sigma_x\sin\theta, \tag{34}$$

where Δ is a positive constant and $\theta\in[0,\pi]$ is the parameter for the extension in the third dimension. With this, we find that the stability of the single Dirac point at $\mathbf{k}=(0,0,0)$ is guaranteed by the invariant (9) with $\mathbf{g}=(\Delta\sin\theta, k\cos\phi\cos\theta, k\sin\phi\cos\theta)$, which evaluates to $n_{M\mathbb{Z}_2}=1$. However, as indicated by the $M\mathbb{Z}_2$-type invariant, a doubled version of this Dirac point is unstable. This can be seen by considering two copies of Hamiltonian (32), i.e., $H_s^{\mathrm{AII}}\otimes\mathbb{1}$. The doubled Dirac point of this 8×8 Hamiltonian can be gapped out by the momentum-independent SPGT $\sigma_x\otimes\sigma_x\otimes\sigma_y$, which is in agreement with the value of the topological number $n_{M\mathbb{Z}_2}=0$ for $H_s^{\mathrm{AII}}\otimes\mathbb{1}$.

$M\mathbb{Z}_2$-type invariants only protect Fermi surfaces of dimension zero ($d_{\mathrm{FS}}=0$) at high-symmetry points of the BZ. To illustrate this, we consider an extension of Hamiltonian (32) to four spatial dimensions with a Fermi line along the fourth momentum direction k_w. This Fermi line, which is located at $(0,0,0,k_w)$, can be gapped out by the symmetry-preserving kinetic term $k_w\sigma_x\otimes\sigma_x$. Only the Fermi point at $(0,0,0,0)$ remains gapless; it is protected by the nonzero $M\mathbb{Z}_2$ invariant which is well defined only for $k_w=0$.

3. *Nodal spin-singlet superconductor with TRS and R_{+-}-type reflection symmetry (class CII with R_{+-} and $p=2$)*

Let us now discuss an example of a nodal superconductor with an $M\mathbb{Z}_2\oplus\mathbb{Z}_2$-type index. According to Table II, point nodes of time-reversal-invariant spin-singlet superconductors with an R_{+-}-type reflection symmetry are protected by an $M\mathbb{Z}_2\oplus\mathbb{Z}_2$ topological invariant. A simple example of such a reflection-symmetric topological superconductor is provided by the 4×4 Hamiltonian

$$H_{\mathrm{s}}^{\mathrm{CII}} = k_x\sigma_y\otimes\mathbb{1} + k_y\sigma_x\otimes\mathbb{1}, \tag{35}$$

which preserves time-reversal and particle-hole symmetry with $T=\sigma_y\otimes\mathbb{1}\mathcal{K}$ and $C=\sigma_x\otimes\sigma_y\mathcal{K}$, respectively. $H_{\mathrm{s}}^{\mathrm{CII}}$ is invariant under reflection $k_x\to -k_x$ with $R=\sigma_x\otimes\sigma_y$. Since $T^2=-\mathbb{1}, C^2=-\mathbb{1}, [T,R]=0$, and $\{C,R\}=0$, Hamiltonian (35) belongs to symmetry class CII with R_{+-}. The two-dimensional superconductor (35) exhibits a point node at $\mathbf{k}=(0,0)$ whose stability is guaranteed by a $M\mathbb{Z}_2\oplus\mathbb{Z}_2$ topological index. To demonstrate this, we compute both the global invariant $n_{\mathbb{Z}_2}$ and the mirror invariant $n_{M\mathbb{Z}_2}$. From Table II, we find that the global invariant $n_{\mathbb{Z}_2}$ in column $p=2$ is a second descendant of a $\mathbb{Z}$-type invariant in column $p=4$. Hence, the topological number $n_{\mathbb{Z}_2}$ can be defined in terms of an extension of $H_{\mathrm{s}}^{\mathrm{CII}}$ to four dimensions [34,35]

$$\begin{aligned}\widetilde{H}_{\mathrm{s}}^{\mathrm{CII}} = {}& [k_x\sigma_y\otimes\mathbb{1} + k_y\sigma_x\otimes\mathbb{1}]\sin\theta\sin\psi \\ & + \sigma_z\otimes\sigma_z\sin\theta\cos\psi + \sigma_z\otimes\sigma_x\cos\theta,\end{aligned} \tag{36}$$

where $\psi,\theta\in[0,\pi]$ are the parameters for the extension to four dimensions. Just as Eq. (35), Hamiltonian (36) satisfies both time-reversal and particle-hole symmetry with

$$T^{-1}\widetilde{H}_{\mathrm{s}}^{\mathrm{CII}}(-\mathbf{k},\pi-\psi,\pi-\theta)T = \widetilde{H}_{\mathrm{s}}^{\mathrm{CII}}(\mathbf{k},\psi,\theta) \tag{37a}$$

and

$$C^{-1}\widetilde{H}_{\mathrm{s}}^{\mathrm{CII}}(-\mathbf{k},\pi-\psi,\pi-\theta)C = -\widetilde{H}_{\mathrm{s}}^{\mathrm{CII}}(\mathbf{k},\psi,\theta), \tag{37b}$$

respectively. We note that for the definition of the *global* invariant $n_{\mathbb{Z}_2}$ we do not need to consider the restrictions imposed by reflection symmetry. Using the extension (36), the $n_{\mathbb{Z}_2}$ invariant is expressed as

$$n_{\mathbb{Z}_2} = \frac{1}{48\pi^2}\oint_{\mathcal{C}}\mathrm{Tr}\left[S\left(\widetilde{H}_{\mathrm{s}}^{\mathrm{CII}}\mathbf{d}[\widetilde{H}_{\mathrm{s}}^{\mathrm{CII}}]^{-1}\right)^3\right]\ \mathrm{mod}\ 2, \tag{38}$$

with the chiral symmetry operator $S=\sigma_z\otimes\sigma_y$ and $\mathcal{C}$ a three-dimensional contour which encloses the point node and which is mapped onto itself by both TRS and PHS [see Fig. 1(a)]. Choosing $\mathcal{C}$ to be the unit three-sphere S^3, we parametrize the momenta as $k_x=\cos\phi$ and $k_y=\sin\phi$, which yields

$$\begin{aligned}n_{\mathbb{Z}_2} = {}& \frac{1}{8\pi^2}\int_0^{2\pi}d\phi\int_0^{\pi}d\psi\int_0^{\pi}d\theta\,\mathrm{Tr}\left[S\left(\widetilde{H}_{\mathrm{s}}^{\mathrm{CII}}\partial_\phi[\widetilde{H}_{\mathrm{s}}^{\mathrm{CII}}]^{-1}\right)\right. \\ & \left.\times\left(\widetilde{H}_{\mathrm{s}}^{\mathrm{CII}}\partial_\psi[\widetilde{H}_{\mathrm{s}}^{\mathrm{CII}}]^{-1}\right)\left(\widetilde{H}_{\mathrm{s}}^{\mathrm{CII}}\partial_\theta[\widetilde{H}_{\mathrm{s}}^{\mathrm{CII}}]^{-1}\right)\right]\ \mathrm{mod}\ 2 = 1,\end{aligned} \tag{39}$$

indicating that the point node at $\mathbf{k}=(0,0)$ is protected by the nontrivial value of $n_{\mathbb{Z}_2}$.

As opposed to the global invariant $n_{\mathbb{Z}_2}$, the mirror invariant $n_{M\mathbb{Z}_2}$ is defined in the reflection plane $k_x=0$ for a given eigenspace of the reflection operator R. Focusing on the eigenspace $R=+1$, we find that the extended Hamiltonian (36) in this eigenspace within the mirror plane is given by

$$\widetilde{h}_{R=+1}^{\mathrm{CII}} = k_y\sigma_y\sin\psi\sin\theta - \sigma_z\cos\psi\sin\theta + \sigma_x\cos\theta, \tag{40}$$

where $\psi\in[0,\pi]$ and $\theta\in[0,\pi]$. Hamiltonian (40) is invariant under TRS:

$$T_R^{-1}\widetilde{h}_{R=+1}^{\mathrm{CII}}(-\mathbf{k},\pi-\psi,\pi-\theta)T_R = \widetilde{h}_{R=+1}^{\mathrm{CII}}(\mathbf{k},\psi,\theta), \tag{41}$$

with $T_R=i\sigma_y\mathcal{K}$. The mirror invariant $n_{M\mathbb{Z}_2}$ is of the same form as Eq. (9) with an integration contour that preserves TRS, that lies within the mirror plane, and that surrounds the nodal point [see Fig. 3(a)]. As the integration contour we choose a two-sphere S^2 which intersects the (k_x,k_y) plane at $\mathbf{k}=(0,\pm a)$, such that the Fermi point at $\mathbf{k}=(0,0)$ on the mirror line is enclosed by $k_y=\pm a$ [see Fig. 3(a)]. That is, to perform the contour integration $k_y=0$ in $\widetilde{h}_{R=+1}^{\mathrm{CII}}$ is replaced by a and ψ is integrated over the interval $[0,2\pi]$, whereas θ is integrated over $[0,\pi]$. With this integration contour we find that $n_{M\mathbb{Z}_2}$ is given by Eq. (9) with $\mathbf{g}=(\cos\theta, a\sin\psi\sin\theta, -\cos\psi\sin\theta)$, which evaluates to $n_{M\mathbb{Z}_2}=1$. Hence, the point node at $\mathbf{k}=(0,0)$ is protected also by the mirror invariant $n_{M\mathbb{Z}_2}$.

As indicated in Table II, $M\mathbb{Z}_2\oplus\mathbb{Z}_2$-type indices only protect Fermi surfaces (superconducting nodes) of dimension

zero, i.e., $d_{\mathrm{FS}} = 0$. To exemplify this, we consider a trivial extension of Hamiltonian (35) to three spatial dimensions by including the extra momentum component k_z, which yields a three-dimensional superconductor with a line node at $(0,0,k_z)$. However, this line node is unstable since it can be gapped out by the symmetry-preserving kinetic term $k_z\sigma_z \otimes \sigma_x$. Only the point node at $\mathbf{k} = (0,0,0)$ is topologically stable. Moreover, we find that the global invariant $n_{\mathbb{Z}_2}$ [Eq. (38)], as well as the mirror invariant $n_{M\mathbb{Z}_2}$, cannot be defined for the three-dimensional superconductor with a line node along the k_z direction since it is impossible to choose a time-reversal-invariant integration contour that surrounds this nodal line (except for $k_z = 0$ and π).

4. Reflection-symmetric nodal spin-singlet superconductor (class C with R_- and $p = 2$)

As a fourth example, we consider a two-dimensional nodal spin-singlet superconductor with reflection symmetry, which is described by the 4×4 Hamiltonian

$$H_{\mathrm{s}}^{\mathrm{C}} = k_x\sigma_x \otimes \sigma_y + k_y\sigma_y \otimes \sigma_y. \tag{42}$$

Equation (42) satisfies PHS with $C = \sigma_y \otimes \mathbb{1}\mathcal{K}$ and is invariant under reflection $k_x \to -k_x$ with $R = \sigma_y \otimes \mathbb{1}$. Because $C^2 = -\mathbb{1}$ and $\{C,R\} = 0$, Hamiltonian (42) belongs to symmetry class C with an R_--type reflection symmetry. This superconductor has a point node at $\mathbf{k} = (0,0)$, which, according to Table II, is protected by a $T\mathbb{Z}_2$ invariant. Indeed, there exists no SPGT that can gap out this point node. To demonstrate the $\mathbb{Z}_2$-type property of Eq. (42), we consider different doubled versions of the Hamiltonian. Using $H_{\mathrm{s}}^{\mathrm{C}}$, there are four possibilities to construct an 8×8 Hamiltonian in the symmetry class C with R_- [12]:

$$H_{++}^{\mathrm{C}} = H_{\mathrm{s}}^{\mathrm{C}} \otimes \mathbb{1}, \qquad H_{--}^{\mathrm{C}} = H_{\mathrm{s}}^{\mathrm{C}} \otimes \sigma_z, \tag{43a}$$

$$H_{-+}^{\mathrm{C}} = k_x\sigma_x \otimes \sigma_y \otimes \mathbb{1} + k_y\sigma_y \otimes \sigma_y \otimes \sigma_z, \tag{43b}$$

and

$$H_{+-}^{\mathrm{C}} = k_x\sigma_x \otimes \sigma_y \otimes \sigma_z + k_y\sigma_y \otimes \sigma_y \otimes \mathbb{1}. \tag{43c}$$

We find that the first three Hamiltonians can be fully gapped out by the momentum-independent SPGTs $\mathbb{1} \otimes \sigma_z \otimes \sigma_y$, $\mathbb{1} \otimes \mathbb{1} \otimes \sigma_y$, and $\sigma_y \otimes \sigma_y \otimes \sigma_y$, respectively. Interestingly, the fourth Hamiltonian H_{+-}^{C} has a stable point node at $\mathbf{k} = 0$, i.e., there exists no SPGT for H_{+-}^{C}. However, if we consider quadrupled versions of $H_{\mathrm{s}}^{\mathrm{C}}$ [Eq. (42)], we find that for each quadrupled Hamiltonian there exists at least one SPGT which gaps out all the point nodes. (In a sense, the Hamiltonian has a $\mathbb{Z}_4$ property rather than a $\mathbb{Z}_2$ property.)

B. Fermi surfaces within mirror planes but off high-symmetry points

Second, we present some examples of Fermi surfaces (superconducting nodes) that are left invariant by the mirror symmetry but transform pairwise into each other under the global symmetries. These Fermi surfaces are located within the mirror plane but away from the time-reversal-invariant momenta [see Fig. 3(b)].

1. Reflection-symmetric Dirac semimetal with TRS (class AII with R_+ and $p = 2$)

We begin by considering the following two-orbital tight-binding Hamiltonian $\mathcal{H}_{\mathrm{n}}^{\mathrm{AII}} = \sum_{\mathbf{k}} \Psi_{\mathbf{k}}^\dagger h_{\mathrm{n}}^{\mathrm{AII}}(\mathbf{k})\Psi_{\mathbf{k}}$, with the spinor $\Psi_{\mathbf{k}} = [\psi_{\uparrow 1}(\mathbf{k}),\psi_{\uparrow 2}(\mathbf{k}),\psi_{\downarrow 1}(\mathbf{k}),\psi_{\downarrow 2}(\mathbf{k})]^{\mathrm{T}}$ and

$$h_{\mathrm{n}}^{\mathrm{AII}}(\mathbf{k}) = t_x \sin k_x\, \sigma_z \otimes \tau_x + [1 - t_y \cos k_y]\sigma_0 \otimes \tau_z, \tag{44}$$

where σ_i operates in spin grading and τ_i in orbital grading [78]. This Hamiltonian satisfies TRS, with $T = \sigma_y \otimes \tau_0\mathcal{K}$, and reflection symmetry $k_x \to -k_x$, with $R = \sigma_0 \otimes \tau_z$. Because $T^2 = -\mathbb{1}$ and $[R,T] = 0$, semimetal (44) belongs to symmetry class AII with R_+. The spectrum of the Hamiltonian is given by

$$E = \pm\sqrt{t_x^2 \sin^2 k_x + (1 - t_y \cos k_y)^2}. \tag{45}$$

For $t_y > 1$, Hamiltonian (44) has four Dirac points at $(k_x,k_y) = (0, \pm \arccos[1/t_y])$ and $(\pi, \pm \arccos[1/t_y])$, for $t_y = 1$ there are two Dirac points at $(k_x,k_y) = (0,0)$ and $(\pi,0)$, and for $t_y < 1$ there is a full gap in the BZ. The reflection symmetry R maps each Dirac point onto itself, i.e., the Fermi points are located within the mirror lines $k_x = 0$ and π [see Fig. 3(b)]. Since there does not exist any SPGT that can be added to Eq. (44), the four Dirac points of Hamiltonian (44) with $t_y > 1$ are topologically stable and protected against gap opening by TRS and reflection symmetry. This is in agreement with the classification of Table II (column $p = 2$), which shows that the Fermi points are protected by a mirror invariant of type $2M\mathbb{Z}$, where the prefix "2" indicates that the mirror invariant only takes on even values. To exemplify this for semimetal (44), we evaluate the mirror number $n_{2M\mathbb{Z}}$ for the reflection line $k_x = 0$. We find that $h_{\mathrm{n}}^{\mathrm{AII}}$ in the eigenspace $R = \pm 1$ for $k_x = 0$ reads as

$$h_{R=\pm 1}^{\mathrm{AII}} = \pm(1 - t_y \cos k_y)\mathbb{1}. \tag{46}$$

The mirror index $n_{2M\mathbb{Z}}^{\pm}$ for the eigenspace $R = \pm 1$ is given by the difference of occupied states (i.e., states with $E < 0$) of Hamiltonian $h_{R=\pm 1}^{\mathrm{AII}}$ on either side of the Dirac point, i.e.,

$$n_{2M\mathbb{Z}}^{\pm} = n_{\mathrm{occ}}^{\pm}(|k_y| < k_0) - n_{\mathrm{occ}}^{\pm}(|k_y| > k_0) = \pm 2, \tag{47}$$

where $k_0 = \arccos[1/t_y]$ and

$$n_{\mathrm{occ}}^{+}(k_y) = \begin{cases} 2, & |k_y| < k_0 \\ 0, & |k_y| > k_0 \end{cases}, \quad n_{\mathrm{occ}}^{-}(k_y) = \begin{cases} 0, & |k_y| < k_0 \\ 2, & |k_y| > k_0 \end{cases} \tag{48}$$

denotes the number of occupied states at $\mathbf{k} = (0,k_y)$ in the eigenspace or R with eigenvalue $+1$ and -1, respectively. Hence, the two Dirac points at $(0, \pm k_0)$ are protected by the invariant (47). The index $n_{2M\mathbb{Z}}$ for the $k_x = \pi$ line, which guarantees the stability of the Fermi points at $(\pi, \pm k_0)$, can be computed in a similar fashion.

2. Reflection-symmetric tight-binding model on the honeycomb lattice (class AI with R_+ and $p = 2$)

As a second example, we discuss a tight-binding model of spinless fermions on the honeycomb lattice, which describes the electronic properties of graphene [79] (ignoring any spin-dependent terms). Considering both first- and second-neighbor hopping, the tight-binding Hamiltonian can be written as

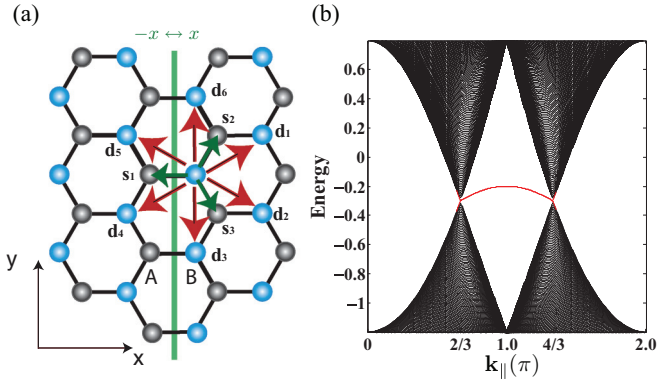

FIG. 4. (Color online) (a) The honeycomb lattice of graphene is a bipartite lattice composed of two interpenetrating triangular sublattices. The two sublattices are marked "A" (black dots) and "B" (blue dots). The nearest-neighbor bond vectors (green arrows) are given by $\mathbf{s}_1 = (-1,0)$, $\mathbf{s}_2 = \frac{1}{2}(1,\sqrt{3})$, and $\mathbf{s}_3 = \frac{1}{2}(1,-\sqrt{3})$. The second-neighbor bond vectors (red arrows) are $\mathbf{d}_1 = -\mathbf{d}_4 = \frac{1}{2}(3,\sqrt{3})$, $\mathbf{d}_2 = -\mathbf{d}_5 = \frac{1}{2}(3,-\sqrt{3})$, and $\mathbf{d}_3 = -\mathbf{d}_6 = (0,-\sqrt{3})$. The mirror line $x \to -x$ is indicated by the green line. (b) Energy spectrum of a graphene ribbon with (10) edges (i.e., zigzag edges) and $(t_1,t_2) = (1.0,0.1)$. A linearly dispersing edge state (red trace) connects the Dirac points, which are located at $k_\parallel = 2\pi/3$ and $4\pi/3$ in the edge BZ and are projected from the bulk Dirac points at $(0, \pm k_0)$.

$\mathcal{H}_{\rm n}^{\rm AI} = \sum_{\mathbf{k}} \Psi_{\mathbf{k}}^\dagger h_{\rm n}^{\rm AI}(\mathbf{k})\Psi_{\mathbf{k}}$ with the spinor $\Psi_{\mathbf{k}} = (a_{\mathbf{k}},b_{\mathbf{k}})^{\rm T}$ and

$$h_{\rm n}^{\rm AI}(\mathbf{k}) = \begin{pmatrix} \Theta_{\mathbf{k}} & \Phi_{\mathbf{k}} \\ \Phi_{\mathbf{k}}^* & \Theta_{\mathbf{k}} \end{pmatrix}, \tag{49}$$

where $a_{\mathbf{k}}$ and $b_{\mathbf{k}}$ denote the fermion annihilation operators with momentum $\mathbf{k}$ on sublattices A and B, respectively. The hopping terms are given by $\Phi_{\mathbf{k}} = t_1 \sum_{i=1}^{3} e^{+i\mathbf{k}\cdot\mathbf{s}_i}$ and $\Theta_{\mathbf{k}} = t_2 \sum_{i=1}^{6} e^{+i\mathbf{k}\cdot\mathbf{d}_i}$, where $\mathbf{s}_i$ and $\mathbf{d}_i$ denote the nearest- and second-neighbor bond vectors, respectively [Fig. 4(a)]. The hopping integrals t_1 and t_2 are assumed to be positive.

Hamiltonian (49) satisfies TRS with $T = \sigma_0\mathcal{K}$ and is invariant under the mirror symmetry $k_x \to -k_x$ with $R = \sigma_x$. [Incidentally, Eq. (49) is also symmetric under $k_y \to -k_y$. However, we shall ignore this symmetry since it does not play any role for the protection of the Dirac points.] Because $T^2 = +\mathbb{1}$ and $[R,T] = 0$, we find that Hamiltonian (49) belongs to symmetry class AI with R_+. The energy spectrum

$$E_{\mathbf{k}}^{\pm} = +2t_2\left[2\cos\left(\frac{3k_x}{2}\right)\cos\left(\frac{\sqrt{3}k_y}{2}\right) + \cos(\sqrt{3}k_y)\right] \pm t_1\left[3 + 4\cos\left(\frac{3k_x}{2}\right)\cos\left(\frac{\sqrt{3}k_y}{2}\right) + 2\cos(\sqrt{3}k_y)\right]^{\frac{1}{2}} \tag{50}$$

exhibits two Dirac points, which are located on the mirror line $k_x = 0$, i.e., at $(k_x,k_y) = (0, \pm k_0)$ in the BZ, with $k_0 = 4\pi/(3\sqrt{3})$. These two Dirac points transform pairwise into each other under TRS. Because there does not exist any SPGT that can be added to Eq. (49), we find that the Dirac points are topologically stable and protected against gap opening by TRS, reflection symmetry, and SU(2) spin-rotation symmetry. In particular, we note that the TRS-preserving mass term σ_3 is forbidden by reflection symmetry R. This finding is confirmed by the classification of Table II, which indicates that the stability of the Dirac points is guaranteed by an $M\mathbb{Z}$-type invariant.

To compute this mirror invariant $n_{M\mathbb{Z}}$, we determine the eigenstates $\psi_{\mathbf{k}}^{\pm}$ of $h_{\rm n}^{\rm AI}(\mathbf{k})$ with energy $E_{\mathbf{k}}^{\pm}$:

$$\psi_{\mathbf{k}}^{-} = \frac{1}{\sqrt{2}}\begin{pmatrix} -e^{i\varphi_{\mathbf{k}}} \\ 1 \end{pmatrix}, \quad \psi_{\mathbf{k}}^{+} = \frac{1}{\sqrt{2}}\begin{pmatrix} e^{i\varphi_{\mathbf{k}}} \\ 1 \end{pmatrix}, \tag{51}$$

where $\varphi_{\mathbf{k}} = \arg[\Phi_{\mathbf{k}}]$. On the mirror line $k_x = 0$ we have

$$e^{i\varphi_{(0,k_y)}} = \begin{cases} +1, & |k_y| < k_0 \\ -1, & |k_y| > k_0. \end{cases} \tag{52}$$

Hence, $\psi_{(0,k_y)}^{\pm}$ are simultaneous eigenstates of the reflection operator $R = \sigma_x$ with opposite eigenvalue ($+1$ or -1), which prohibits the hybridization between them. The mirror invariant $n_{M\mathbb{Z}}^{\pm}$ is given by the difference of the number of states with energy $E_{\mathbf{k}}^{-}$ and reflection eigenvalue $R = \pm 1$ on either side of the Dirac point, i.e.,

$$n_{M\mathbb{Z}}^{\pm} = n_{\rm neg}^{\pm}(|k_y| > k_0) - n_{\rm neg}^{\pm}(|k_y| < k_0), \tag{53}$$

where $n_{\rm neg}^{\pm}(k_y)$ denotes the number of states with energy $E_{\mathbf{k}}^{-}$ and reflection eigenvalue $R = \pm 1$. Using Eq. (52), we find that $n_{M\mathbb{Z}}^{\pm} = \pm 1$, and hence the Dirac points are protected by the mirror invariant (53). By the bulk-boundary correspondence, the nontrivial topology of the Dirac points leads to a linearly dispersing edge mode, which connects the projected Dirac points in the (10) edge BZ [see Fig. 4(b)].

3. *Reflection-symmetric semimetal with Fermi rings (class A with R and p = 3)*

To exemplify that $M\mathbb{Z}$-type invariants can give rise to topologically stable Fermi surfaces with $d_{\rm FS} > 0$, we consider the following three-dimensional semimetal on the square lattice $\mathcal{H}_{\rm n}^{\rm A} = \sum_{\mathbf{k}} \Psi_{\mathbf{k}}^\dagger h_{\rm n}^{\rm A}(\mathbf{k})\Psi_{\mathbf{k}}$, with the spinor $\Psi_{\mathbf{k}} = [c_1(\mathbf{k}),c_2(\mathbf{k}),c_3(\mathbf{k}),c_4(\mathbf{k})]^{\rm T}$ and

$$h_{\rm n}^{\rm A}(\mathbf{k}) = M(\mathbf{k})\tau_0 \otimes \sigma_z + m_2\tau_z \otimes \sigma_z + \sin k_x \tau_0 \otimes \sigma_x. \tag{54}$$

Here, $M(\mathbf{k}) = m_1 - \cos k_x - \cos k_y - \cos k_z$ is a momentum-dependent mass term, and m_1 and m_2 are positive constants. Equation (54) breaks both TRS and PHS, but is symmetric under $k_x \to -k_x$ with $R = \tau_0 \otimes \sigma_z$. Incidentally, Eq. (54) also exhibits a chiral symmetry with $S = \mathbb{1} \otimes \sigma_y$ and $\{R,S\} = 0$, which corresponds to class AIII with R_- in Table II. However, chiral symmetry can be broken by including a staggered chemical potential

$$V_s = \mu_s \sum_{i=1}^{N} (-1)^i \Psi^\dagger(x_i)\mathbb{1} \otimes \sigma_y \Psi_y(x_i), \tag{55}$$

with N the number of lattice sites in the x direction. For simplicity, we assume that N is an even number. The Hamiltonian with the staggered chemical potential, i.e., $\mathcal{H}_{\rm n}^{\rm A} + V_s$, is still reflection symmetric about the mirror plane $x = (x_1 + x_N)/2$, and hence belongs to class A with R in Table II.

The energy spectrum of $\mathcal{H}_{\rm n}^{\rm A}$ in the absence of V_s is given by

$$E_{\pm,\mu} = \pm\sqrt{[M + (-1)^\mu m_2]^2 + \sin^2 k_x}, \tag{56}$$

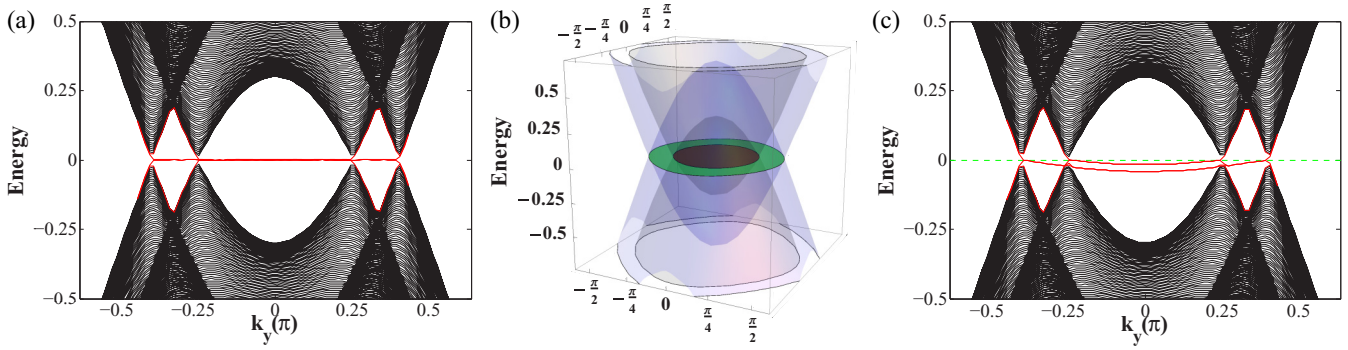

FIG. 5. (Color online) (a) Surface band structure of semimetal (54) for the (100) face with $\mu_s = 0$, $k_z = 0$, $m_1 = 2.5$, and $m_2 = 0.2$ as a function of surface momentum k_y. Note that the (100) surface is not symmetric under $k_x \to -k_x$. Zero-energy surface flat bands (red traces) appear within regions of the surface BZ that are bounded by the projected bulk Fermi lines. (b) Surface spectrum on the (100) face as a function of both k_y and k_z for the same parameters as in panel (a). Nondegenerate zero-energy flat bands protected by the winding number $n_{\mathbb{Z}} = 1$ [see Eq. (62)] appear within the region $1.3 < \cos k_y + \cos k_z < 1.7$ of the surface BZ (green area). Doubly degenerate flat bands protected by $n_{\mathbb{Z}} = 2$ exist within the region $\cos k_y + \cos k_z > 1.7$ (brown area). (c) Surface spectrum in the presence of a staggered chemical potential (55) with $\mu_s = 0.05$. Linearly dispersing surface states (red traces) connect the projected Fermi rings in the surface BZ.

with $\mu \in \{1,2\}$. Assuming that $m_2 > 0$ and $m_1 - m_2 > 1$, we find that Hamiltonian (54) exhibits two Fermi rings (i.e., two Fermi surfaces with $d_{\rm FS} = 1$) located within the mirror plane $k_x = 0$, which are described by

$$\cos k_y + \cos k_z = m_1 - 1 \pm m_2. \tag{57}$$

These Fermi rings are topologically stable since there does not exist any reflection-symmetric mass term nor any reflection-symmetric kinetic term that can be added to Eq. (54) (cf. Appendix A). This finding is in agreement with Table II, which shows that the Fermi rings (57) are protected by an $M\mathbb{Z}$-type invariant (in the presence of V_s) or an $M\mathbb{Z} \oplus \mathbb{Z}$-type invaraint (in the absence of V_s). To demonstrate this, let us compute the corresponding mirror and winding numbers.

The mirror number $n_{M\mathbb{Z}}$ is defined within the mirror plane $k_x = 0$ for a given eigenspace of the reflection operator R. Focusing on the eigenspace $R = +1$, we find that $h^{\rm A}_{\rm n}(0,k_y,k_z)$ in this subspace reads as

$$h^{\rm A}_{R=+1} = (m - 1 - \cos k_y - \cos k_z)\mathbb{1} - m_2\sigma_z. \tag{58}$$

The mirror topological number $n_{M\mathbb{Z}}$ is given by the difference of occupied states (i.e., states with negative energy) on either side of the Fermi ring

$$n^+_{M\mathbb{Z}} = n^+_{\rm occ}(k_y^>,k_z^>) - n^+_{\rm occ}(k_y^<,k_z^<), \tag{59}$$

where $(k_y^>,k_z^>)$ and $(k_y^<,k_z^<)$ are two momenta on either side of the Fermi ring and

$$n^+_{\rm occ}(k_y,k_z) = \begin{cases} 2, & \widetilde{m}(k_y,k_z) < -m_2 \\ 1, & -m_2 < \widetilde{m}(k_y,k_z) < +m_2 \\ 0, & \widetilde{m}(k_y,k_z) > +m_2 \end{cases} \tag{60}$$

with $\widetilde{m}(k_y,k_z) = m_1 - 1 - \cos k_y - \cos k_z$, represents the number of occupied states in the eigenspace with $R = +1$.

In the absence of the staggered chemical potential V_s, Hamiltonian (54) satisfies chiral symmetry and the Fermi rings are also protected by a winding number $n_{\mathbb{Z}}$, which takes the form of Eq. (12) with

$$\mathbf{q} = \begin{pmatrix} \frac{\sin k_x - i[M(\mathbf{k})+m_2]}{r_+} & 0 \\ 0 & \frac{\sin k_x - i[M(\mathbf{k})-m_2]}{r_-} \end{pmatrix}, \tag{61}$$

where $r_\pm = \sqrt{[M(\mathbf{k}) \pm m_2]^2 + \sin^2 k_x}$, and an integration contour $\mathcal{C}$ that encircles the Fermi ring. Choosing the contour along the k_x direction we find

$$n_{\mathbb{Z}}(k_y,k_z) = \begin{cases} 2, & \widetilde{m}(k_y,k_z) < -m_2 \\ 1, & -m_2 < \widetilde{m}(k_y,k_z) < +m_2 \\ 0, & \widetilde{m}(k_y,k_z) > +m_2. \end{cases} \tag{62}$$

By the bulk-boundary correspondence, a nontrivial value of $n_{\mathbb{Z}}$ [Eq. (62)] leads to zero-energy flat bands at the surface of the semimetal. These zero-energy states appear within regions of the surface BZ that are bounded by the projection of the bulk Fermi rings [see Figs. 5(a) and 5(b)]. When chiral symmetry is broken, for example by a finite staggered chemical potential V_s, the surface flat bands acquire a finite dispersion [see Fig. 5(c)].

4. *Unstable reflection-symmetric nodal superconductors (class DIII with R_{-+} and $p = 2$, class D with R_+ and $p = 2$)*

As shown in Table II, $\mathbb{Z}_2$-type topological invariants (i.e., $\mathbb{Z}_2$, $M\mathbb{Z}_2$, and $M\mathbb{Z}_2 \oplus \mathbb{Z}_2$) do not protect Fermi surfaces (superconducting nodes) that are located within the mirror planes but away from high-symmetry points (cf. Sec. II A 2 c). However, these $\mathbb{Z}_2$-type invariants can lead to protected gapless surface states. To exemplify this behavior, we study in this section two-dimensional unstable nodal superconductors belonging to class DIII with R_{-+}-type reflection and class D with R_+-type reflection, which are classified as $M\mathbb{Z}_2 \oplus \mathbb{Z}_2$ and $M\mathbb{Z}_2$, respectively, in Table II. For this purpose, we borrow an example from Sec. II A 2 c, i.e., $\mathcal{H}^{\rm DIII}_{\rm n} = \sum_{\mathbf{k}} \Psi^\dagger_{\mathbf{k}} h^{\rm DIII}_{\rm n} \Psi_{\mathbf{k}}$ with the Nambu spinor $\Psi_{\mathbf{k}} = (a^\dagger_{\mathbf{k}}, b^\dagger_{\mathbf{k}}, a_{-\mathbf{k}}, b_{-\mathbf{k}})^{\rm T}$ and

$$h^{\rm DIII}_{\rm n} = (1 + \cos k_x + \cos k_y)\sigma_x \otimes \sigma_y + \sin k_x \sigma_y \otimes \mathbb{1}, \tag{63}$$

which describes a time-reversal-symmetric superconductor with point nodes located at $(\pi, \pm\pi/2)$. Here, $a^\dagger_{\mathbf{k}}$ and $b^\dagger_{\mathbf{k}}$

represent fermionic creation operators with momentum $\mathbf{k}$. Hamiltonian (63) preserves TRS and PHS with $T = \sigma_y \otimes \mathbb{1}\mathcal{K}$ and $C = \sigma_x \otimes \mathbb{1}\mathcal{K}$, respectively, and is invariant under $k_x \to -k_x$ with $R = \sigma_x \otimes \mathbb{1}$. Because $T^2 = -\mathbb{1}$, $C^2 = +\mathbb{1}$, $\{R,T\} = 0$, and $[R,C] = 0$, Eq. (63) belongs to class DIII with R_{-+}. According to Table II, the point nodes of Hamiltonian (63), which transform pairwise into each other by TRS and PHS, are topologically unstable, even though the topological numbers $n_{\mathbb{Z}_2}$ [cf. Eq. (17)] and $n_{M\mathbb{Z}_2}$ for Hamiltonian (63) take on nontrivial values. Indeed, we find that the symmetry-preserving extra kinetic term $\delta t \sin k_y \sigma_x \otimes \sigma_x$ gaps out the Fermi points at $(\pi, \pm\pi/2)$ and turns Eq. (63) into a fully gapped reflection-symmetric topological superconductor

$$\mathcal{H}^{\mathrm{DIII}}_{\mathrm{fg}} = \mathcal{H}^{\mathrm{DIII}}_{\mathrm{n}} + \delta t \sum_{\mathbf{k}} \Psi^\dagger_{\mathbf{k}} \sin k_y \sigma_x \otimes \sigma_x \Psi_{\mathbf{k}}. \tag{64}$$

That is, the unstable nodal superconductor (63) is connected to the fully gapped reflection-symmetric topological superconductor (64) and inherits topological edge states from the fully gapped phase [72].

To demonstrate this, let us compute the global $n_{\mathbb{Z}_2}$ invariant and the mirror invariant $n_{M\mathbb{Z}_2}$ for Hamiltonians (63) and (64). The computation of the global invariant $n_{\mathbb{Z}_2}$, which is given by Eq. (17), follows along similar lines as in the example of Sec. II A 2 c. (Note that for the definition of a $\mathbb{Z}_2$-type invariant the reflection symmetry does not play any role; the $\mathbb{Z}_2$ number $n_{\mathbb{Z}_2}$ is defined solely in terms of the global symmetries.) We find that for a contour $\mathcal{C}$ oriented along the k_x axis with k_y held fixed at $k_y = 0$ (or $k_y = \pi$), the topological index evaluates to $n_{\mathbb{Z}_2} = +1$ (or $n_{\mathbb{Z}_2} = -1$) both for the nodal superconductor $\mathcal{H}^{\mathrm{DIII}}_{\mathrm{n}}$ and the fully gapped superconductor $\mathcal{H}^{\mathrm{DIII}}_{\mathrm{fg}}$. This indicates that there appear zero-energy edge states at $k_y = \pi$ of the (10) edge BZ of both the fully gapped and the nodal systems.

To calculate the mirror number $n_{M\mathbb{Z}_2}$ we focus on the eigenspace of the reflection operator with eigenvalue $R = +1$ and transform Hamiltonian (64) to a Majorana basis [80]. On the mirror lines $k_x = 0$ and π, $\mathcal{H}^{\mathrm{DIII}}_{\mathrm{fg}}$ in the eigenspace $R = +1$ can be expressed as

$$\mathcal{H}^{\mathrm{DIII},\nu}_{R=+1} = \sum_{k_y} M_\nu(k_y) \begin{pmatrix} d^\dagger_{\nu,k_y} & d_{\nu,-k_y} \end{pmatrix} \begin{pmatrix} 1 & -i\delta T \\ i\delta T & -1 \end{pmatrix} \begin{pmatrix} d_{\nu,k_y} \\ d^\dagger_{\nu,-k_y} \end{pmatrix}, \tag{65}$$

with $\nu \in \{0,\pi\}$ and where $M_\nu(k_y) = 1 + (-1)^{\nu/\pi} + \cos k_y$ and $\delta T(k_y) = \delta t \sin k_y$. In Eq. (65), the transformed fermion operators d_{ν,k_y} are given by

$$d_{\nu,k_y} = \tfrac{1}{2}[a^\dagger_{\nu,k_y} + a_{\nu,-k_y} - i(b^\dagger_{\nu,k_y} + b_{\nu,-k_y})]. \tag{66}$$

Using Eq. (66) we can construct real Majorana operators $\Lambda_{\nu,k_y} = (\lambda_{\nu,k_y}, \lambda'_{\nu,k_y})^{\mathrm{T}}$, with

$$\lambda_{\nu,k_y} := d^\dagger_{\nu,k_y} + d_{\nu,k_y}, \quad \lambda'_{\nu,k_y} := i(d^\dagger_{\nu,-k_y} - d_{\nu,-k_y}), \tag{67}$$

and rewrite the Hamiltonian in the $R = +1$ eigenspace as

$$\mathcal{H}^{\mathrm{DIII},\nu}_{R=+1} = \frac{i}{2} \sum_{k_y} \Lambda^{\mathrm{T}}_{\nu,-k_y} B_\nu(k_y) \Lambda_{\nu,k_y}, \tag{68a}$$

with

$$B_\nu(k_y) = \begin{pmatrix} \delta T(k_y) & M_\nu(k_y) \\ -M_\nu(k_y) & \delta T(k_y) \end{pmatrix}. \tag{68b}$$

It follows that the mirror invariant $n_{M\mathbb{Z}_2}$ on the two mirror lines $k_y = 0$ and π is given by

$$n^\nu_{M\mathbb{Z}_2} = \mathrm{sgn}[\mathrm{Pf}\, B_\nu(0)]\mathrm{sgn}[\mathrm{Pf}\, B_\nu(\pi)] = \begin{cases} +1, & \nu = 0 \\ -1, & \nu = \pi. \end{cases} \tag{69}$$

Interestingly, the value of $n^\nu_{M\mathbb{Z}_2}$ does not depend on the extra kinetic term $\delta t \sin k_y \sigma_x \otimes \sigma_x$. Hence, we conclude that the unstable nodal superconductor $\mathcal{H}^{\mathrm{DIII}}_{\mathrm{n}}$ can be connected to the fully gapped topological superconductor $\mathcal{H}^{\mathrm{DIII}}_{\mathrm{fg}}$ (whose bulk topology is described by $n^0_{M\mathbb{Z}_2} n^\pi_{M\mathbb{Z}_2}$) without changing the values of the invariants $n_{\mathbb{Z}_2}$ and $n^\nu_{M\mathbb{Z}_2}$. Both $n_{\mathbb{Z}_2}$ and $n^\nu_{M\mathbb{Z}_2}$ lead to protected zero-energy states at the edge of the nodal (or fully gapped) superconductor.

We observe that in systems that are classified as $M\mathbb{Z}_2 \oplus \mathbb{Z}_2$ in Table II the two invariants $n_{M\mathbb{Z}_2}$ and $n_{\mathbb{Z}_2}$ always take on the same values. This is in contrast to topological materials with an $M\mathbb{Z} \oplus \mathbb{Z}$ classification, where the two invariants $n_{M\mathbb{Z}}$ and $n_{\mathbb{Z}}$ can be distinct (see example in Sec. IV A 1). That is, the presence of reflection symmetry in $M\mathbb{Z}_2 \oplus \mathbb{Z}_2$-type systems does not lead to any new topological characteristics, but it simplifies the calculation of the topological index, i.e., the topological characteristics can be inferred from the wave functions at reflection planes alone. (This situation is in a sense similar to the $\mathbb{Z}_2$ time-reversal-symmetric topological insulator with inversion symmetry of Ref. [81], where the inversion symmetry does not lead to new topological features, but simplifies the formula for the topological index.)

A similar analysis as above can be preformed for a two-dimensional unstable nodal superconductor in class D with R_+-type reflection symmetry. In the absence of TRS, the global $\mathbb{Z}_2$ number $n_{\mathbb{Z}_2}$ is ill defined, however, the mirror invariant $n_{M\mathbb{Z}_2}$ is still well defined and takes on nontrivial values (cf. Table II). This mirror index leads to stable zero-energy modes at edges that are invariant under reflection. As before, we find that a reflection-symmetric nodal superconductor in class D with R_+ can be connected to a fully gapped topological superconductor without removing the zero-energy edge states.

5. *Reflection-symmetric nodal spin-triplet superconductor with TRS (class DIII with R_{--} and $p = 3$)*

As the last example of this section, we study a three-dimensional reflection-symmetric superconductor in class DIII:

$$h^{\mathrm{DIII}}_{\mathrm{3D}} = M(\mathbf{k})\sigma_z \otimes \mathbb{1} + \sin k_x \sigma_x \otimes \sigma_x + \sin k_z \sigma_x \otimes \sigma_z, \tag{70}$$

which exhibits point nodes at $\mathbf{k} = (0, \pm\pi/3, 0)$. The k-dependent mass $M(\mathbf{k})$ is given by $M(\mathbf{k}) = -2.5 + \cos k_x + \cos k_y + \cos k_z$. Hamiltonian (70) satisfies TRS and PHS with $T = \mathbb{1} \otimes \sigma_y \mathcal{K}$ and $C = \sigma_x \otimes \mathbb{1}\mathcal{K}$, respectively, and is reflection symmetric under $k_x \to -k_x$ with $R = \sigma_z \otimes \sigma_x$. Because $T^2 = -\mathbb{1}$, $C^2 = +\mathbb{1}$, $\{T,R\} = 0$, and $\{C,R\} = 0$, Eq. (70) is classified as DIII with R_{--}. The two point nodes, which are located within the mirror plane at $\mathbf{k} = (0, \pm\pi/3, 0)$, are protected by TRS, PHS, and reflection symmetry since there does not exist any SPGT that can be added to Eq. (70).

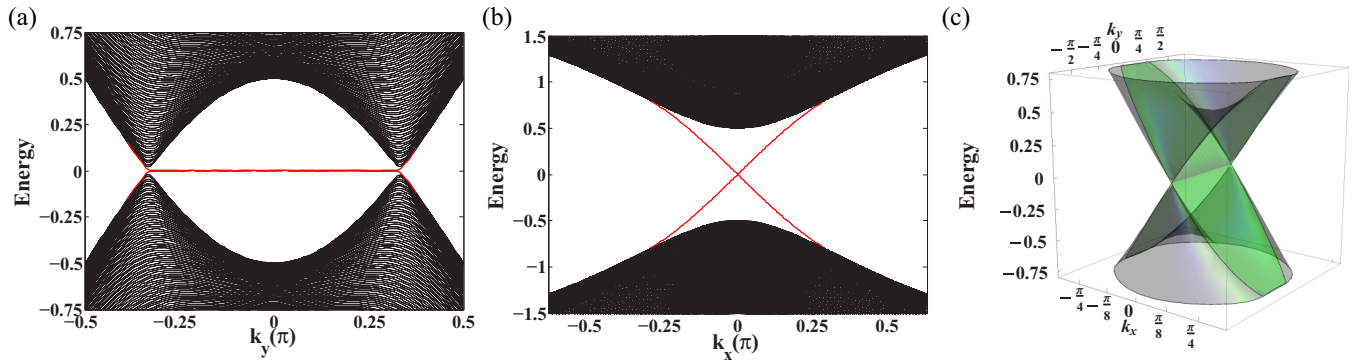

FIG. 6. (Color online) Surface band structure of the reflection-symmetric nodal superconductor (70) (class DIII with R_{--}) for the (001) face as a function of (a) surface momentum k_y with $k_x = 0$ and (b) surface momentum k_x with $k_y = 0$. A zero-energy arc surface state (red trace) connects the projected point nodes in the surface BZ. (c) Surface spectrum on the (001) face as a function of both k_x and k_y. The surface states and bulk states are indicated in green and gray, respectively.

We note that the gap-opening term $\sin k_y \sigma_y \otimes \mathbb{1}$ is symmetric under TRS and PHS but breaks mirror symmetry, which shows that the reflection symmetry R is crucial for the protection of the point nodes. Indeed, as indicated by Table I, the point nodes are unstable in the absence of reflection symmetry.

Let us now compute the mirror invariant $n_{M\mathbb{Z}}$ which, as listed in Table II, protects the point nodes. Since the chiral symmetry operator $S = TC = \sigma_x \otimes \sigma_y$ commutes with R, the mirror number $n_{M\mathbb{Z}}$ can be expressed as a one-dimensional winding number, i.e., for the eigenspace $R = +1$ it takes the form of Eq. (12) with

$$\mathbf{q} = \frac{M(\mathbf{k}) - \sin k_z i}{\sqrt{M(\mathbf{k})^2 + \sin^2 k_z}}, \tag{71}$$

and a contour $\mathcal{C}$ that lies within the mirror plane and encloses one of the point nodes [see Fig. 3(b)]. Choosing the contour along the k_z axis with $k_x = 0$ and k_y a fixed parameter, we find that the mirror number evaluates to

$$n^{+}_{M\mathbb{Z}}(k_y) = \begin{cases} 1, & 0 \leqslant |k_y| < \frac{\pi}{3} \\ 0, & \frac{\pi}{3} < |k_y| \leqslant \pi. \end{cases} \tag{72}$$

By the bulk-boundary correspondence, the nontrivial value of Eq. (72) leads to zero-energy arc states on surfaces that are perpendicular to the mirror plane. As shown in Fig. 6, these zero-energy arc states connect two projected point nodes in the surface BZ.

C. Fermi surfaces outside mirror planes

Third, we discuss three examples of Fermi surfaces (superconducting nodes) that lie outside the mirror plane. These Fermi surfaces are pairwise related to each other by both reflection and nonspatial symmetries [see Fig. 3(c)]. Their topological properties are classified by Table III.

1. *Reflection-symmetric Dirac semimetal with TRS (class AII with R_+ and $p = 3$)*

We start by studying an example of a three-dimensional Dirac semimetal with an R_+-type reflection symmetry, which is described by [75,78,82]

$$H^{\mathrm{AII}}_{\mathrm{off}} = \sin k_y \tau_x \otimes \sigma_z + \sin k_z \tau_y \otimes \mathbb{1} + \mathcal{M}(\mathbf{k}) \tau_z \otimes \mathbb{1}. \tag{73}$$

Here, $\mathcal{M}(\mathbf{k}) = M - \cos k_x - \cos k_y - \cos k_z$ and M is a positive constant, which we set to $M = 2.0$. The Pauli matrices σ_i and τ_i operate in spin and orbital gradings, respectively. Hamiltonian (73) preserves TRS with $T = \mathbb{1} \otimes i\sigma_y \mathcal{K}$ and is symmetric under $k_x \to -k_x$ with $R = \mathbb{1} \otimes \mathbb{1}$. Since $T^2 = -\mathbb{1}$ and $[T, R] = 0$, the Hamiltonian belongs to class AII with R_+. By computing the energy spectrum, we find that the semimetal exhibits two doubly degenerate Dirac points that are located outside the reflection plane $k_x = 0$, i.e., at $\mathbf{k} = (\pm\pi/2, 0, 0)$. These Fermi points are protected by a combination of time-reversal and reflection symmetries because there does not exist any SPGT that can be added to Eq. (73). We note, however, that in the absence of reflection symmetry, the Dirac points can be gapped out by the time-reversal-invariant term $\sin k_x \tau_x \otimes \sigma_x$, which turns Hamiltonian (73) into a class AII topological insulator. This finding is in agreement with the tenfold classification of gapless topological materials shown in Table I. To determine whether the Dirac points have a $\mathbb{Z}$- or $\mathbb{Z}_2$-type character, we consider a doubled version of $H^{\mathrm{AII}}_{\mathrm{off}}$, i.e., $H^{\mathrm{AII}}_{\mathrm{off}} \otimes \mathbb{1}$. For the doubled Hamiltonian, there exists a momentum-independent SPGT (i.e., $\tau_x \otimes \sigma_x \otimes \sigma_y$), demonstrating that the Dirac points are protected by a $\mathbb{Z}_2$-type invariant, which is denoted as "$C\mathbb{Z}_2$" in Table III.

The $C\mathbb{Z}_2$ invariant $n_{C\mathbb{Z}_2}$ is defined in terms of the combined symmetry (26b), i.e., $\tilde{T}^{-1} H^{\mathrm{AII}}_{\mathrm{off}}(k_x, -\tilde{\mathbf{k}}) \tilde{T} = H^{\mathrm{AII}}_{\mathrm{off}}(k_x, \tilde{\mathbf{k}})$. Since each plane perpendicular to the k_x axis is left invariant by the combined symmetry (26b), we can define the topological number $n_{C\mathbb{Z}_2}$ for any given plane E_{k_x} with fixed k_x [see Fig. 3(c)]. We find that

$$n_{C\mathbb{Z}_2}(k_x) = \begin{cases} +1, & \frac{\pi}{2} < |k_x| \leqslant \pi \\ -1, & 0 \leqslant |k_x| < \frac{\pi}{2}. \end{cases} \tag{74}$$

Due to the bulk-boundary correspondence, the nontrivial value of $n_{C\mathbb{Z}_2}(k_x)$ in the interval $[-\pi/2, +\pi/2]$ gives rise to helical Fermi arcs on surfaces that are perpendicular to the reflection plane [75,82]. These helical arc states connect the project bulk Dirac points in the surface BZ.

2. Reflection-symmetric nodal spin-triplet superconductor (class D with R_- and $d = 3$)

Next, we consider a reflection-symmetric nodal spin-triplet superconductor, which is described by the BdG Hamiltonian

$$H^{\mathrm{D}}_{\mathrm{off}} = \sin k_y \tau_y \otimes \sigma_z + \sin k_z \tau_x \otimes \sigma_z + \mathcal{M}(\mathbf{k})\tau_z \otimes \mathbb{1}, \quad (75)$$

where $\mathcal{M}(\mathbf{k}) = 2 - \cos k_x - \cos k_y - \cos k_z$. Here, the Pauli matrices σ_i and τ_i act in spin and particle-hole space, respectively. $H^{\mathrm{D}}_{\mathrm{off}}$ satisfies PHS with $C = \tau_x \otimes \mathbb{1}\mathcal{K}$ and is invariant under $k_x \to -k_x$ with $R_- = \tau_z \otimes \sigma_x$. Because $C^2 = +\mathbb{1}$ and $\{R, C\} = 0$, the BdG Hamiltonian belongs to class D with R_-. As an aside, we note that reflection symmetry $k_x \to -k_x$ for spin-$\frac{1}{2}$ systems is usually implemented by the operator $R'_{\mathrm{p}} = +i\sigma_x$ ($R'_{\mathrm{h}} = -i\sigma_x$) for particlelike (holelike) degrees of freedom, i.e., by the operator $R' = i\tau_z \otimes \sigma_x$ in particle-hole space. However, in order to correctly categorize the Hamiltonian with respect to the 27 symmetry classes of Table III, we need to ensure that the reflection operator R is Hermitian [cf. Eq. (20)]. Therefore, we have dropped the factor i in the above definition of R.

The spectrum of Hamiltonian (75) exhibits two doubly degenerate point nodes, which are located outside the mirror plane at $\mathbf{k} = (\pm\pi/2, 0, 0)$. These point nodes are topologically stable since there does not exist any SPGT that can be added to Eq. (75). According to Table III, the point nodes of $H^{\mathrm{D}}_{\mathrm{off}}$ are protected by an invariant of type "$2\mathbb{Z}$" (i.e., a Chern number), where the prefix "2" indicates that the topological number only takes on even values. Choosing the two-dimensional integration contour to be a plane perpendicular to the k_x axis, we find that the Chern number for Hamiltonian (75) is given by

$$\begin{aligned} n_{\mathbb{Z}}(k_x) &= \frac{i}{2\pi} \int \sum_{i=1}^{2} d\langle u_i^- | d u_i^- \rangle \\ &= -\int \frac{1}{2\pi R^3} \big(Z dX \wedge dY + X dY \wedge dZ + Y dZ \wedge dX \big), \end{aligned} \quad (76)$$

where $X = \sin k_z$, $Y = \sin k_y$, $Z = \mathcal{M}(\mathbf{k})$, and $R = \sqrt{X^2 + Y^2 + Z^2}$. Evaluating the integral, we obtain

$$n_{\mathbb{Z}}(k_x) = \begin{cases} 0, & \frac{\pi}{2} < |k_x| \leqslant \pi \\ -2, & 0 \leqslant |k_x| < \frac{\pi}{2}. \end{cases} \quad (77)$$

Note that for the definition of the Chern number (77), the combined symmetry $\tilde{C} = RC$ [Eq. (26c)] does not not play any role, except to ensure that there are an even number of point nodes on either side of the reflection planes. By the bulk-boundary correspondence, the nontrivial value of $n_{\mathbb{Z}}$ [Eq. (77)] gives rise to arc surface states which connect the projected point nodes in the surface BZ [62].

3. Unstable reflection-symmetric nodal superconductor with TRS (class DIII with R_{-+} and $d = 2$)

As stated in Sec. III D 4, superconducting nodes outside the mirror plane in systems of class DIII with R_{-+}-type reflection symmetry are unstable, even though a nontrivial $M\mathbb{Z}_2$-type invariant can be defined for these systems. To illustrate this, we consider the following BdG Hamiltonian:

$$H^{\mathrm{DIII}}_{\mathrm{off}} = \sin k_y \sigma_x \otimes \mathbb{1} + (1 + \cos k_x + \cos k_y)\sigma_z \otimes \sigma_y, \quad (78)$$

which describes a superconductor with unstable point nodes. Equation (78) preserves TRS and PHS with $T = \sigma_y \otimes \mathbb{1}\mathcal{K}$ and $C = \sigma_x \otimes \sigma_z \mathcal{K}$, respectively, and is symmetric under $k_x \to -k_x$ with $R = \sigma_x \otimes \sigma_z$. Because $T^2 = -\mathbb{1}$, $C^2 = +\mathbb{1}$, $\{T, R\} = 0$, and $[C, R] = 0$, Hamiltonian (78) is classified as DIII with R_{-+}. We find that the spectrum of Eq. (78) exhibits point nodes located away from the mirror lines $k_x = 0$ and π, i.e., at $\mathbf{k} = (\pm\pi/2, 0, 0)$. These point nodes are topologically unstable since there exists a momentum-dependent SPGT (i.e., $\sin k_x \sigma_y \otimes \mathbb{1}$), which opens up a full gap.

Let us now examine topological invariants for Hamiltonian (78). First, we consider a winding number $\nu_{\mathbb{Z}}$, which is defined by chiral symmetry with $S = TC = -i\sigma_z \otimes \sigma_z$ on a line perpendicular to the k_x direction. Since chiral symmetry is momentum independent, combining reflection and chiral symmetries is not required to define the winding number $\nu_{\mathbb{Z}}$. We find that this one-dimensional winding number is given by Eq. (5) with

$$q = \frac{1}{\sqrt{\sin^2 k_y + M^2}} \begin{pmatrix} \sin k_y & -iM \\ -iM & \sin k_y \end{pmatrix}, \quad (79)$$

where $M = 1 + \cos k_x + \cos k_y$. Evaluating the integral, one obtains that $\nu_{\mathbb{Z}}$ is trivial for any fixed k_x (i.e., $\nu_{\mathbb{Z}} = 0$), in agreement with the fact that the point nodes are unstable. Second, we consider the mirror invariant, which is defined within the mirror lines $k_x = 0$ and π for a given eigenspace of R. Since $H^{\mathrm{DIII}}_{\mathrm{off}}$ restricted to the mirror lines satisfies PHS, a mirror invariant of type $M\mathbb{Z}_2$ can be defined. By a similar calculation as in example Sec. IV B 4, we find that the mirror invariant $n_{M\mathbb{Z}_2}$ is given by $n_{M\mathbb{Z}_2} = 1$ for $k_x = 0$ and $n_{M\mathbb{Z}_2} = -1$ for $k_x = \pi$. However, even though $n_{M\mathbb{Z}_2}$ takes on a nontrivial value, this $M\mathbb{Z}_2$-type invariant does not protect the point nodes that are located at $\mathbf{k} = (\pm\pi/2, 0)$ (see Appendix C 3).

V. SUMMARY AND CONCLUSIONS

In this paper, we have performed an exhaustive classification of reflection-symmetry-protected topological semimetals and nodal superconductors. We have shown that the classification depends on (i) the codimension $p = d - d_{\mathrm{FS}}$ of the Fermi surface (nodal line) of the semimetal (nodal superconductor), (ii) how the Fermi surface (nodal line) transforms under the crystal reflection and the global symmetries, and (iii) whether the reflection-symmetry operator R commutes or anticommutes with the global (i.e., nonspatial) symmetries. The result of this classification scheme is summarized in Tables II and III, which show that the presence of reflection symmetries leads to an enrichment of the tenfold classification of gapless topological materials (cf. Table I) with additional topological states. The reflection symmetry R together with the three nonspatial symmetries, time-reversal, particle-hole, and chiral symmetry, define a total of 27 different symmetry classes. For Fermi surfaces with even (odd) codimension p located within the mirror plane, 17 (10) out of these 27 classes allow for nontrivial topological characteristics of the Fermi surface (Table II). For Fermi surfaces located outside the

mirror plane, on the other hand, there are 9 symmetry classes which permit the existence of nontrivial topological properties (Table III).

To illustrate the general principles of the classification schemes, we have discussed in Sec. IV concrete examples of reflection-symmetry-protected topological semimetals and nodal superconductors. The topological properties of these gapless materials manifest themselves at the surface in the form of linearly dispersing Dirac or Majorana modes, or dispersionless states, which form two-dimensional flat bands or one-dimensional arcs (see Figs. 4, 5, and 6). These different types of surface states are protected by different types of topological invariants. For the examples of Sec. IV we have derived explicit expressions for these topological numbers.

Probably, the most prominent example of a reflection-symmetric topological semimetal is graphene [79], whose Dirac points are protected against gap opening by time-reversal symmetry together with reflection and SU(2) spin-rotation symmetry. In the classification scheme of Table II, graphene belongs to class AI with R_+-type reflection symmetry. Hence, the Dirac points of graphene, which are located within the reflection line but away from time-reversal-invariant points, are protected by a mirror invariant ($M\mathbb{Z}$) (see Sec. IV B 2). The classifications of Tables II and III predict several new reflection-symmetric topological semimetals and nodal superconductors, for which realistic physical systems have yet to be found. For example, a reflection-symmetric topological nodal superconductor with spin-triplet pairing is predicted to exist in three spatial dimensions (class DIII with R_{--}) (see Sec. IV B 5). This nodal superconductor, which exhibits two point nodes within the reflection plane (but away from the time-reversal-invariant momenta), is a three-dimensional superconducting analog of graphene.

Recently, several examples of space-group symmetry-protected topological semimetals have been theoretically proposed [83,84]. The surface states of Na_3Bi [85–87] and Cd_3As_2 [88–90], which are two topological Dirac materials protected by rotation symmetry, have been experimentally observed using angle-resolved photoemission and scanning tunneling measurements. We hope that these recent discoveries will spur the experimental search for other types of topological phases. The results of this paper will be useful for the search and design of new gapless topological materials that are protected by reflection symmetry.

ACKNOWLEDGMENTS

The authors thank G. Bian, M. Franz, M. Garcia Vergniory, P. Horsch, S. Ryu, and A. Yaresko for useful discussions. The support of the Max-Planck-UBC Centre for Quantum Materials is gratefully acknowledged. A.P.S. wishes to thank the ESI (Vienna) for its hospitality.

APPENDIX A: REVIEW OF TENFOLD CLASSIFICATION SCHEME OF GAPLESS TOPOLOGICAL MATERIALS

Topological properties of gapless materials can be classified by two different methods [26,33–35]: (i) the minimal Dirac-matrix Hamiltonian method and (ii) the derivation of topological invariants. For the former, the topological property is determined by the existence or nonexistence of a symmetry-preserving gap-opening term (SPGT). The existence of an SPGT implies trivial topology of the gapless system, i.e., the Fermi surface (nodal line) is topologically unstable. In the absence of such an SPGT, however, the gapless state is topologically nontrivial and exhibits topologically stable Fermi surfaces (nodal lines). Method (i) is similar to the approach of Refs. [12,74], which classify fully gapped topological materials by studying symmetry-preserving extra mass terms that allow us to deform different gapped states into each other without closing the bulk gap. Method (ii), on the other hand, relies on the existence or nonexistence of nonzero topological invariants. A nonzero topological invariant implies nontrivial topology of the gapless quantum system. In this Appendix and in Appendix C, we use the minimal Dirac-matrix Hamiltonian approach [i.e., method (i)] to derive the topological classification of gapless materials. These derivations should be compared to the discussions in the main text, which uses the topological-invariant approach [i.e., method (ii)]; see, in particular, Sec. III D.

1. Fully gapped materials

Before discussing the tenfold classification of gapless materials (cf. Table I), let us briefly state some results and definitions related to the tenfold classification of fully gapped systems. The Dirac Hamiltonian ($H^{\mathrm{TI}}_{\mathrm{Dirac}}$) that classifies fully gapped systems (i.e., topological insulators and superconductors) is given by Eq. (22), where the Dirac matrices γ_i are kinetic terms and the Dirac matrices $\tilde{\gamma}_j$ represent mass terms. For real symmetry classes, these Dirac matrices obey

$$\{T,\gamma_i\}=0, \quad [C,\gamma_i]=0, \tag{A1}$$

$$[T,\tilde{\gamma}_j]=0, \quad \{C,\tilde{\gamma}_j\}=0, \tag{A2}$$

to preserve TRS and PHS. Note that both Dirac matrices γ_i and $\tilde{\gamma}_j$ anticommute with the chiral symmetry operator $S=CT$. The classification of fully gapped topological materials follows from the homotopy groups, which are given by [6,12,74]

$$K^{\mathbb{C}}(s,d)=\pi_0(\mathcal{C}_{s-d}), \tag{A3a}$$

$$K^{\mathbb{R}}(s,d)=\pi_0(\mathcal{R}_{s-d}), \tag{A3b}$$

where $\mathcal{C}_s$ and $\mathcal{R}_s$ denote the complex and real classifying spaces, respectively. Equations (A3) are in line with the existence or nonexistence of symmetry-allowed kinetic terms (γ_i) and mass terms ($\tilde{\gamma}_j$) which enter in the minimal-Dirac matrix description (see Table IV). In the case, where the classification is trivial, which is labeled by "0" in Table IV, the symmetry-preserving mass term $m\tilde{\gamma}_1$ in $H^{\mathrm{TI}}_{\mathrm{Dirac}}$ allows us to deform different gapped phases into each other without closing the bulk gap. Hence, in this case there is only one topological equivalence class, namely, the trivial one. When there is a binary classification, which is labeled by "$\mathbb{Z}_2$" in Table IV, there exists an extra symmetry-allowed kinetic term $k_j\gamma_{d+1}$ that can be added to $H^{\mathrm{TI}}_{\mathrm{Dirac}}$. This kinetic term allows us to deform the doubled version of $H^{\mathrm{TI}}_{\mathrm{Dirac}}$ to a trivial state without closing the bulk gap. Finally, in the case of the $\mathbb{Z}$ classification,

TABLE IV. This table lists the presence or absence of symmetry-allowed kinetic terms (γ_i) or mass terms ($\tilde{\gamma}_j$) for each of the 10 Altland-Zirnbauer symmetry classes. Due to the periodicity of two and eight for complex and real symmetry classes, respectively, $l = 0,1$ mod 2 for $\mathcal{C}_l$ and $l = 0,1,\ldots,7$ mod 8 for $\mathcal{R}_l$.

s	AZ class ($d = 0$)	Topological invariant	Gamma matrix
0	A	$\pi_0(\mathcal{C}_0) = \mathbb{Z}$	
1	AIII	$\pi_0(\mathcal{C}_1) = 0$	γ_{d+1} or $\tilde{\gamma}_1$
0	AI	$\pi_0(\mathcal{R}_0) = \mathbb{Z}$	
1	BDI	$\pi_0(\mathcal{R}_1) = \mathbb{Z}_2$	γ_{d+1}
2	D	$\pi_0(\mathcal{R}_2) = \mathbb{Z}_2$	γ_{d+1}, γ_{d+2}
3	DIII	$\pi_0(\mathcal{R}_3) = 0$	γ_{d+1}, γ_{d+2}, γ_{d+3}
4	AII	$\pi_0(\mathcal{R}_4) = 2\mathbb{Z}$	
5	CII	$\pi_0(\mathcal{R}_5) = 0$	$\tilde{\gamma}_1$, $\tilde{\gamma}_2$, $\tilde{\gamma}_3$
6	C	$\pi_0(\mathcal{R}_6) = 0$	$\tilde{\gamma}_1$, $\tilde{\gamma}_2$
7	CI	$\pi_0(\mathcal{R}_7) = 0$	$\tilde{\gamma}_1$

both symmetry-allowed kinetic terms (γ_i) and mass terms ($\tilde{\gamma}_j$) are absent.

2. Gapless materials

The classification of global symmetry-invariant Fermi points is related to the tenfold classification of fully gapped systems by the dimensional shift $d \to d-1$ (see Table I). In other words, the classification of gapless materials follows from the homotopy groups [26,33–35]

$$G_{\mathrm{s}}^{\mathbb{C}}(s,d) = \pi_0(\mathcal{C}_{s-d-1}), \tag{A4a}$$

$$G_{\mathrm{s}}^{\mathbb{R}}(s,d) = \pi_0(\mathcal{R}_{s-d-1}). \tag{A4b}$$

Equations (A4) are in agreement with the results from the minimal Dirac-matrix Hamiltonian method, which we will discuss in the following. Let us consider a Dirac Hamiltonian describing a Fermi point at a time-reversal-invariant momentum of the BZ (i.e., at $k = 0$)

$$H_{\mathrm{s}}^{\mathrm{Dirac}} = \sum_{i}^{d} k_i \gamma_i. \tag{A5}$$

We note that this Hamiltonian is identical to the fully gapped Dirac Hamiltonian in Eq. (22), except for the mass term $m\tilde{\gamma}_0$. For real symmetry classes, the Dirac matrices γ_i (i.e., the kinetic term) obey Eqs. (A1). Furthermore, we observe that $H_{\mathrm{s}}^{\mathrm{Dirac}}$ in d dimensions can be viewed as the boundary states of $H_{\mathrm{Dirac}}^{\mathrm{TI}}$ in $d+1$ dimensions [see Eq. (23)]. In other words, the Hamiltonian $H_{\mathrm{Dirac}}^{\mathrm{TI}}$ in $d+1$ dimensions is obtained from the d-dimensional Hamiltonian $H_{\mathrm{s}}^{\mathrm{Dirac}}$ by adding an extra kinetic term (i.e., $k_{d+1}\gamma_{d+1}$) and a mass term (i.e., $M\tilde{\gamma}_0$). With this, both $H_{\mathrm{Dirac}}^{\mathrm{TI}}$ and $H_{\mathrm{s}}^{\mathrm{Dirac}}$ satisfy the same global symmetries. The extra symmetry-preserving mass term $m\tilde{\gamma}_1$ that can (or cannot) be added to $H_{\mathrm{Dirac}}^{\mathrm{TI}}$ plays the role of an SPGT that can (or cannot) be added to $H_{\mathrm{s}}^{\mathrm{Dirac}}$. That is, the existence of nonexistence of the term $m\tilde{\gamma}_1$ determines the topology for both $H_{\mathrm{Dirac}}^{\mathrm{TI}}$ and $H_{\mathrm{s}}^{\mathrm{Dirac}}$. Following, we will provide more detail and also show how the minimal Dirac-matrix Hamiltonian approach allows us to distinguish between $\mathbb{Z}_2$ and $\mathbb{Z}$ classifications.

But, before doing so, let us add some remarks about the classification of Fermi surfaces that are located away from high-symmetry points in the BZ. These gapless materials are described by Hamiltonian (24) and their $(d-p)$-dimensional Fermi surfaces are located at the momenta described by Eq. (25). We can interpret Eq. (24) as a $(p-1)$-dimensional fully gapped Hamiltonian with mass term

$$\left(1 - p + \sum_{i=1}^{p} \cos k_i\right) \tilde{\gamma}_0. \tag{A6}$$

[This mass term corresponds to the term $m\tilde{\gamma}_0$ in $H_{\mathrm{Dirac}}^{\mathrm{TI}}$, Eq. (22).] Hence, the classification of Fermi surfaces with codimension p is related to the tenfold classification of topological insulators and superconductor in $(p-1)$ dimensions (see Table I). We note, however, that as opposed to $H_{\mathrm{Dirac}}^{\mathrm{TI}}$, Eq. (24) can be gapped by two different SPGTs, namely, by the mass term $\tilde{\gamma}_1$ *and* by the kinetic term $\sin k_p \gamma_p$. For symmetry classes with a $\mathbb{Z}_2$-type invariant, the SPGT $\sin k_p \gamma_p$ is always allowed by symmetry, whereas for classes with a $\mathbb{Z}$-type number this term is symmetry forbidden. Hence, $\mathbb{Z}_2$-type invariants cannot protect Fermi surfaces located away from high-symmetry points of the BZ. Nevertheless, because these $\mathbb{Z}_2$-type numbers are well defined in $(p-1)$-dimensional planes in the BZ that are invariant under PHS or TRS, nonzero $\mathbb{Z}_2$ numbers can lead to the appearance of gapless surfaces states at high-symmetry points of the surface BZ.

a. Topological invariant "0"

Let us now discuss in more detail the different SPGTs that can be added to the Dirac Hamiltonian (A5). First of all, if any SPGTs exist, then $H_{\mathrm{s}}^{\mathrm{Dirac}}$ belongs to the trivial phase. That is, the Fermi surface is topologically unstable since the spectrum can be gapped by the SPGT without breaking any symmetries. This case is denoted by the label "0" in Table I. For example, consider the following two-dimensional Dirac Hamiltonian in class D:

$$H_{\mathrm{s}}^{\mathrm{D}} = k_x \sigma_x + k_y \sigma_y, \tag{A7}$$

which describes a superconductor with a point node at $\mathbf{k} = (0,0)$. Hamiltonian (A7) preserves PHS with $C = \sigma_x \mathcal{K}$. The nodal point at $\mathbf{k} = (0,0)$ is topologically unstable since the spectrum can be gapped by the SPGT $m\sigma_z$.

If there does not exist any SPGT, then $H_{\mathrm{s}}^{\mathrm{Dirac}}$ is either classified by a $\mathbb{Z}_2$ or a $\mathbb{Z}$ number. To distinguish between $\mathbb{Z}_2$ and $\mathbb{Z}$ classifications, we need to consider doubled versions of $H_{\mathrm{s}}^{\mathrm{Dirac}}$ and then check whether there exist any SPGTs for the doubled Hamiltonian.

b. Topological invariant "$\mathbb{Z}_2$"

A doubled version of $H_{\mathrm{s}}^{\mathrm{Dirac}}$ can be obtained in several different ways. In general, it can be written as

$$\mathcal{H}_2 = \sum_i k_{n_i} \gamma_{n_i} \otimes \sigma_z + \sum_{\mathrm{remain}} k_{n_j} \gamma_{n_j} \otimes \mathbb{1}. \tag{A8}$$

Here, the first summation is over an arbitrary set of γ_{n_i} ($n_i \subseteq \{1,2,\ldots,d-1,d\}$) and the second summation is over γ_{n_j}'s that are not picked up by the first summation. We observe that the enlarged Dirac matrices entering in the definition of $\mathcal{H}_2$

all anticommute with each other and satisfy the same global symmetries as the original Hamiltonian H_s^{Dirac}. Now, if for each choice of the set n_i there exists an SPGT that can be added to $\mathcal{H}_2$, then the Hamiltonian exhibits a $\mathbb{Z}_2$ classification. SPGTs for $\mathcal{H}_2$ can be constructed by considering even and odd numbers of terms in the first summation of Eq. (A8) separately. For an odd number of terms, the SPGTs are given by $\mathfrak{M}$ (or $i\mathfrak{M}$), with $\mathfrak{M} = m(\prod_{n_i}^{\text{odd}} \gamma_{n_i}) \otimes \sigma_u$, where the Pauli matrix $\sigma_u \in \{\sigma_x,\sigma_y\}$ has to be chosen such that $\mathfrak{M}$ (or $i\mathfrak{M}$) preserves TRS and/or PHS. (The choice between $\mathfrak{M}$ and $i\mathfrak{M}$ is determined by the condition that the SPGT is Hermitian.) For an even number of terms in the first sum of Eq. (A8), the SPGTs are given by $\mathfrak{M}$ (or $i\mathfrak{M}$) with $\mathfrak{M} = m(\gamma_{d+1} \prod_{n_i}^{\text{even}} \gamma_{n_i}) \otimes \sigma_u$. As before, $\sigma_u \in \{\sigma_x,\sigma_y\}$ has to be chosen such that PHS and/or TRS is preserved. Note that this formula is always well defined since, according to Table IV, there always exist a γ_{d+1} term for systems with $\mathbb{Z}_2$-type invariants.

To make this more explicit, let us consider the following example of a two-dimensional Dirac Hamiltonian with TRS:

$$h_s^{\text{AII}} = k_x\sigma_x + k_y\sigma_y, \tag{A9}$$

which describes a topological semimetal with a Fermi point at $\mathbf{k} = (0,0)$. The time-reversal-symmetry operator is given by $T = i\sigma_y\mathcal{K}$. Since $T^2 = -\mathbb{1}$, Hamiltonian (A9) belongs to symmetry class AII. We observe that h_s^{AII} is identical to the surface Hamiltonian of a three-dimensional topological insulator with spin-orbit coupling. The only possible mass term, which anticommutes with h_s^{AII}, is σ_z. However, σ_z breaks TRS and is therefore forbidden by symmetry. Hence, h_s^{AII} describes a topologically stable Fermi point. Next, we examine different doubled versions of h_s^{AII}, i.e.,

$$H_s^{\text{AII}} = \begin{pmatrix} h_s^{\text{AII}} & 0 \\ 0 & h_s^{\text{AII}'} \end{pmatrix}, \tag{A10}$$

with $h_s^{\text{AII}'} \in \{h_{s++}^{\text{AII}}, h_{s--}^{\text{AII}}, h_{s+-}^{\text{AII}}, h_{s-+}^{\text{AII}}\}$, where $h_{s\pm\pm}^{\text{AII}} = \pm k_x\sigma_x \pm k_y\sigma_y$ and $h_{s\pm\mp}^{\text{AII}} = \pm k_x\sigma_x \mp k_y\sigma_y$. It is not difficult to show that for each of the four versions of H_s^{AII} there exists at least one SPGT. For example, for h_{s++}^{AII} the SPGT is $\sigma_z \otimes \sigma_y$. Thus, the Fermi point described by H_s^{AII} is unstable. Therefore, we conclude that Eq. (A9) exhibits a $\mathbb{Z}_2$ topological characteristic.

c. Topological invariant "$\mathbb{Z}(2\mathbb{Z})$"

For systems with a $\mathbb{Z}$ (or $2\mathbb{Z}$) topological invariant, there does not exist any SPGT both for H_s^{Dirac} and some of its doubled versions [cf. Eq. (A8)]. To be more specific, when the first summation in Eq. (A8) includes an *odd* number of γ_{n_i}'s, there exists SPGTs, which open up a gap [i.e., $\mathfrak{M}$ or $i\mathfrak{M}$, with $\mathfrak{M} = m(\prod_{n_i}^{\text{odd}} \gamma_{n_i}) \otimes \sigma_u$.] However, when there is an *even* number of γ_{n_i}'s in the first summation of Eq. (A8), an SPGT does not exist due to the absence of an extra kinetic term (γ_{d+1}). It is important to note that two gapless modes are only protected if the two blocks in Eq. (A8) have the same sign. Similarly, the system can be extended to n gapless modes with the same sign in each block. In the absence of an SPGT these n gapless modes are protected. This behavior reveals the signature of the $\mathbb{Z}$ invariant.

For concreteness, let us consider the Hamiltonian of a Weyl semimetal [47,48] as an example. This two-dimensional system, which does not preserve any symmetry, belongs to class A. One of the simplest Hamiltonians, which is also a minimal Dirac-matrix Hamiltonian, can be written as

$$h_s^{\text{A}} = k_x\sigma_x + k_y\sigma_y + k_z\sigma_z. \tag{A11}$$

It is impossible to find an extra gap term because only three Dirac matrices can be present in the 2×2 matrix dimension. Therefore, the gapless mode is stable. To distinguish between $\mathbb{Z}$ and $\mathbb{Z}_2$ classification, we need to consider two copies of h_s^{A}. One doubled version of h_s^{A} is given by

$$H_s^{\text{A}} = k_x\sigma_x \otimes \sigma_z + k_y\sigma_y \otimes \mathbb{1} + k_z\sigma_z \otimes \mathbb{1}. \tag{A12}$$

We find that there are two SPGTs that can be added to H_s^{A}, i.e., $\sigma_x \otimes \sigma_x$ and $\sigma_x \otimes \sigma_y$. Hence, the gapless modes of H_s^{A} are unstable. However, there exists another doubled version of h_s^{A}, namely,

$$H_s^{\text{A}'} = k_x\sigma_x \otimes \mathbb{1} + k_y\sigma_y \otimes \mathbb{1} + k_z\sigma_z \otimes \mathbb{1}. \tag{A13}$$

There does not exist any SPGT that can be added to $H_s^{\text{A}'}$, so the two identical gapless modes of $H_s^{\text{A}'}$ are stable. Since there exists one doubled version of h_s^{A} which has two protected gapless modes, we conclude that the system exhibits a $\mathbb{Z}$ classification.

APPENDIX B: CLASSIFICATION OF REFLECTION-SYMMETRY-PROTECTED TOPOLOGICAL INSULATORS AND FULLY GAPPED SUPERCONDUCTORS

As discussed in Sec. III, the classification of reflection-symmetry-protected semimetals (nodal superconductors) can be related to the classification of reflection-symmetry-protected insulators (fully gapped superconductors) by dimensional reduction. To make this relation more explicit, we briefly survey in this Appendix the classification of fully gapped topological materials protected by crystal reflection symmetries [12,13,26]. This classification scheme crucially depends on whether the crystal reflection symmetry commutes or anticommutes with the global nonspatial symmetries.

The classification of reflection-symmetry-protected topological insulators and fully gapped superconductors is summarized in Table II, where the first row indicates the dimension d of the fully gapped system [12,13,26]. In even (odd) spatial dimension d, 10 (17) out of the 27 symmetry classes allow for the existence of nontrivial topological insulators/superconductors protected by reflection symmetry. The different topological sectors within a given class of reflection-symmetry-protected topological insulators/superconductors can be labeled by an integer $\mathbb{Z}$ number, a binary $\mathbb{Z}_2$ quantity, a mirror Chern or winding number $M\mathbb{Z}$, a mirror binary $\mathbb{Z}_2$ quantity $M\mathbb{Z}_2$, or a binary $\mathbb{Z}_2$ quantity with translation symmetry $T\mathbb{Z}_2$. Interestingly, reflection-symmetric topological states belonging to symmetry classes with chiral symmetry can be protected in some cases by both an integer $\mathbb{Z}$ number (binary $\mathbb{Z}_2$ quantity) and a mirror Chern or winding number $M\mathbb{Z}$ (mirror $\mathbb{Z}_2$ quantity $M\mathbb{Z}_2$), as indicated by the label $M\mathbb{Z} \oplus \mathbb{Z}$ ($M\mathbb{Z}_2 \oplus \mathbb{Z}_2$) in Table II. The nontrivial bulk topology characterized by these invariants manifests itself at the boundary in terms of protected Dirac or Majorana surface states, which, depending on the type of the invariant, appear either at any surface (for $\mathbb{Z}$ and $\mathbb{Z}_2$)

or only at surfaces that are left invariant under the reflection symmetry (for $M\mathbb{Z}$ and $M\mathbb{Z}_2$). As explained in Sec. III, by use of a dimensional reduction procedure, these surface states of a d-dimensional fully gapped system can be interpreted as a reflection-symmetry-protected topological semimetal (or nodal superconductor) in $d-1$ dimensions.

Before discussing in detail the different invariants that characterize reflection-symmetry-protected topological materials, we remark that the recently discovered topological crystalline insulator SnTe is included in Table II [28–31]. Specifically, SnTe belongs to symmetry class AII with $T^2=-\mathbb{1}$ in $d=3$ dimensions and exhibits a reflection symmetry R_- that anticommutes with the time-reversal-symmetry operator T. As indicated by Table II, this crystalline topological insulator is described by a mirror Chern number $M\mathbb{Z}$ and hence supports Dirac-cone states at reflection-symmetric surfaces. These Dirac surface states have recently been observed in angle-resolved photoemission experiments [28,30,31].

1. $M\mathbb{Z}$ and $M\mathbb{Z}_2$ invariants

The mirror Chern or winding numbers and mirror $\mathbb{Z}_2$ invariants, denoted by $M\mathbb{Z}$ and $M\mathbb{Z}_2$ in Table II, respectively, are defined on the hyperplanes in the BZ that are symmetric under reflection R, i.e., the two hyperplanes $k_1=0$ and π. Since R is Hermitian and anticommutes with the Hamiltonian $H(\mathbf{k})$ restricted to the hyperplanes $k_1=0$ and π, $H(\mathbf{k})|_{k_1=0,\pi}$ can be block-diagonalized with respect to the two eigenspaces $R=\pm1$ of the reflection operator. We observe that each of the two blocks of $H(\mathbf{k})|_{k_1=0,\pi}$ is left invariant only under those global symmetries that commute with the reflection operator R. Hence, depending on the nonspatial symmetries of the $R=\pm1$ blocks of $H(\mathbf{k})|_{k_1=0,\pi}$, it is possible to define a mirror Chern or winding invariant [12]

$$\nu_{M\mathbb{Z}}=\operatorname{sgn}\left[\nu^{d-1}_{k_1=0}-\nu^{d-1}_{k_1=\pi}\right]\left(\left|\nu^{d-1}_{k_1=0}\right|-\left|\nu^{d-1}_{k_1=\pi}\right|\right), \tag{B1}$$

where $\nu^{d-1}_{k_1=0(\pi)}$ denotes the Chern or winding number of the $R=+1$ block of $H(\mathbf{k})|_{k_1=0(\pi)}$ [91]. Similarly, the mirror $\mathbb{Z}_2$ quantity $M\mathbb{Z}_2$ is defined by

$$n_{M\mathbb{Z}_2}=1-\left|n^{d-1}_{k_1=0}-n^{d-1}_{k_1=\pi}\right|, \tag{B2}$$

with $n^{d-1}_{k_1=0(\pi)}\in\{-1,+1\}$ the $\mathbb{Z}_2$ invariant of the $R=+1$ block of $H(\mathbf{k})|_{k_1=0(\pi)}$. A nontrivial value of these mirror indices indicates the appearance of Dirac or Majorana states at reflection-symmetric surfaces, i.e., at surfaces that are perpendicular to the reflection hyperplane $x_1=0$. At surfaces that break reflection symmetry, however, the boundary modes are in general gapped. Some illustrative examples of topological crystalline insulators with mirror Chern or winding numbers have been discussed in Ref. [12].

2. $\mathbb{Z}$ and $\mathbb{Z}_2$ invariants

For symmetry classes with at least one nonspatial symmetry that anticommutes with the reflection operator R, it is possible in certain cases to define a global $\mathbb{Z}$ or $\mathbb{Z}_2$ number even in the presence of reflection. These $\mathbb{Z}$ and $\mathbb{Z}_2$ indices are identical to the ones of the original tenfold classification in the absence of mirror symmetry (cf. Table I) and lead to the appearance of linearly dispersing Dirac or Majorna states at any surface, independent of the surface orientation.

3. $M\mathbb{Z}\oplus\mathbb{Z}$ and $M\mathbb{Z}_2\oplus\mathbb{Z}_2$ invariants

Topological properties of reflection-symmetric insulators (superconductors) with chiral symmetry are described in some cases by both a global $\mathbb{Z}$ or $\mathbb{Z}_2$ invariant and a mirror index $M\mathbb{Z}$ or $M\mathbb{Z}_2$. The global invariant and the mirror invariant are independent of each other. At surfaces which are perpendicular to the mirror plane, the number of protected gapless states is given by $\max\{|n_{\mathbb{Z}}|,|n_{M\mathbb{Z}}|\}$ [12], where $n_{\mathbb{Z}}$ denotes the global $\mathbb{Z}$ invariant, whereas $n_{M\mathbb{Z}}$ is the mirror $\mathbb{Z}$ invariant. This should be compared to Sec. IV A 1, where we provide an example of a gapless topological phases with nontrivial $M\mathbb{Z}$ and $\mathbb{Z}$ invariants. Examples of gapless topological phases with nontrivial $M\mathbb{Z}_2$ and $\mathbb{Z}_2$ invariants are given in Secs. IV A 3 and IV B 4.

4. $T\mathbb{Z}_2$ invariant

In symmetry classes where the reflection operator R anticommutes with the global antiunitary symmetries TRS and PHS (R_- and R_{--} in Table II), the second descendant $\mathbb{Z}_2$ invariants [8] are only well defined in the presence of translation symmetry. That is, the edge or surface states of these phases can be gapped out by density-wave-type perturbations, which preserve reflection and global symmetries but break translation symmetry. Hence, these topological states are protected by a combination of reflection, translation, and global antiunitary symmetries. Therefore, we denote their topological indices by "$T\mathbb{Z}_2$" in Table II.

To exemplify the properties of reflection-symmetric insulators (superconductors) with a $T\mathbb{Z}_2$ invariant, we consider a two-dimensional superconductor with R_{--} reflection symmetry in class CII given by the 8×8 BdG Hamiltonian

$$H^{\mathrm{CII}}_{\mathrm{bulk}}=M\gamma_0+\sin k_x\gamma_1+\sin k_y\gamma_2, \tag{B3}$$

where $M=1+\cos k_x+\cos k_y$, $\gamma_0=\sigma_z\otimes\mathbb{1}\otimes\mathbb{1}$, $\gamma_1=\sigma_x\otimes\sigma_x\otimes\mathbb{1}$, and $\gamma_2=\sigma_x\otimes\sigma_y\otimes\sigma_x$. Superconductor (B3) preserves TRS and PHS with $T_{\mathrm{bulk}}=\mathbb{1}\otimes\sigma_y\otimes\mathbb{1}\mathcal{K}$ and $C_{\mathrm{bulk}}=\sigma_x\otimes\mathbb{1}\otimes\sigma_y\mathcal{K}$, respectively. Reflection symmetry is implemented as $R^{-1}_{\mathrm{bulk}}H^{\mathrm{CII}}_{\mathrm{bulk}}(-k_x,k_y)R_{\mathrm{bulk}}=H^{\mathrm{CII}}_{\mathrm{bulk}}(k_x,k_y)$, with $R_{\mathrm{bulk}}=\mathbb{1}\otimes\sigma_y\otimes\mathbb{1}$. This topological crystalline superconductor is characterized by a $T\mathbb{Z}_2$ invariant (cf. Table II), which indicates that the helical Majorana states at the (01) edge are only stable in the presence of translation symmetry. We find that these Majorana-cone edge states appear at $k_x=\pm\delta$ of the edge BZ and are described by the following edge Hamiltonian [92]:

$$h^{\mathrm{CII}}_{\mathrm{edge}}=k_x\,\sigma_x\otimes\sigma_x+\delta\,\sigma_z\otimes\sigma_y. \tag{B4}$$

The edge Hamiltonian satisfies TRS, PHS, and reflection symmetry with $T_{\mathrm{edge}}=\sigma_y\otimes\mathbb{1}\mathcal{K}$, $C_{\mathrm{edge}}=\sigma_y\otimes\sigma_z\mathcal{K}$, and $R_{\mathrm{edge}}=\sigma_z\otimes\mathbb{1}$, respectively. In the absence of reflection symmetry, the gap-opening mass term $m\,\sigma_x\otimes\sigma_y$, which preserves both TRS and PHS, can be added to Eq. (B4). Therefore, Hamiltonian (B3) is topologically trivial according to the tenfold classification of Table I. However, with reflection and translation symmetry, $h^{\mathrm{CII}}_{\mathrm{edge}}$ cannot be gapped since $m\,\sigma_x\otimes\sigma_y$

breaks reflection symmetry R_{edge}. Considering two copies of the edge Hamiltonian, i.e., $H^{\text{CII}}_{\text{edge}} = h^{\text{CII}}_{\text{edge}} \otimes \mathbb{1}$, we find that the symmetry-preserving mass term $m\sigma_z \otimes \sigma_x \otimes \sigma_y$ opens up a gap in the spectrum of the doubled Hamiltonian $H^{\text{CII}}_{\text{edge}}$. Hence, BdG Hamiltonian (B3) exhibits a nontrivial $\mathbb{Z}_2$-type topological characteristic (cf. Appendix A 2 b). To demonstrate that the two Majorana edge modes [Eq. (B4)] are unstable against translation symmetry breaking we consider the density-wave-type mass term

$$\hat{\mathfrak{M}} = m \sum_{-\eta \leqslant k_x < \eta} (i c^\dagger_{k_x+\eta+\delta}\, \mathfrak{M}\, c_{k_x-\eta+\delta} + i c^\dagger_{-k_x+\eta-\delta}\, \mathfrak{M}\, c_{-k_x-\eta-\delta} + \text{H.c.}), \tag{B5}$$

which is invariant under TRS, PHS, and reflection $\hat{R} = \sum_{k_x} c^\dagger_{-k_x} \sigma_z \otimes \mathbb{1}\, c_{k_x}$. In Eq. (B5), $\mathfrak{M} = m\sigma_x \otimes \sigma_y$ and η is a constant with $0 < \eta < \delta$. For $m > \eta$, the translation-symmetry-breaking mass term (B5) fully gaps out all edge modes.

In closing, we remark that for the classification of gapless topological materials presented in Sec. III, the presence of translation symmetry is always assumed. In particular, density-wave-type mass terms are disregarded since these can gap out the bulk by coupling Fermi surfaces (nodal lines) located at different parts of the BZ. Thus, the distinction between $\mathbb{Z}_2$ and $T\mathbb{Z}_2$ invariants is irrelevant for the topological classification of reflection-symmetric semimetals and nodal superconductors.

APPENDIX C: CLASSIFICATION OF FERMI POINTS OUTSIDE MIRROR PLANES

In this Appendix, we derive the classification scheme of Table III using the Dirac-matrix Hamiltonian approach. This should be compared to the discussion in Sec. III D, where this classification is derived by examining different types of topological invariants. As in the main text we assume that reflection symmetry maps $k_1 \to -k_1$. To derive the classification, we consider the following reflection-symmetric Dirac-matrix Hamiltonian:

$$H_{\text{off}} = \sum_{i=2}^{d} \sin k_i \gamma_i + \left(1 - d + \sum_{i=1}^{d} \cos k_i\right) \tilde{\gamma}_0, \tag{C1}$$

which describes a d-dimensional gapless system with Fermi points located at

$$\mathbf{k} = (\pm\pi/2, 0, \ldots, 0). \tag{C2}$$

Reflection symmetry acts on Hamiltonian (C1) as $[R, H_{\text{off}}] = 0$. We note that the Fermi surface (C2) lies outside the mirror plane $k_1 = 0$ and away from the high-symmetry points of the BZ. Furthermore, observe that by fixing k_1 to $k_1^0 \neq \pm\pi/2$, Hamiltonian (C1) can be viewed as a $(d-1)$-dimensional insulator

$$H^{d-1}_{\text{off}} = \sum_{i=2}^{d} \sin k_i \gamma_i + \tilde{m}\tilde{\gamma}_0, \tag{C3}$$

with mass $\tilde{m} = (1 - d + \cos k_1^0 + \sum_{i=2}^{d} \cos k_i)$.

In order to classify the Fermi surfaces described by Eq. (C1), two different types of SPGTs need to be considered, i.e.,

$$m\tilde{\gamma}_1 \quad \text{and} \quad \sin k_1 \gamma_1. \tag{C4}$$

The latter is a kinetic term. It will lead to a classification pattern which is quite different from the tenfold classification. Let us now discuss for which of the 27 symmetry classes listed in Table III there exist topologically stable Fermi points.

1. R_+ and R_{++}

We start by considering the case where the reflection operator R commutes with all global symmetries. For simplicity, we can choose $R = \mathbb{1}$. We note that even if the global symmetries allow the kinetic mass term $\sin k_1 \gamma_1$, the reflection symmetry forbids this term due to $k_1 \to -k_1$. Therefore, the classification is solely determined by the presence or absence of the regular mass term $m\tilde{\gamma}_1$. Thus, the classification of d-dimensional gapless modes described by Eq. (C1) is identical to the classification of $(d-1)$-dimensional fully gapped systems [described by Eq. (C3)] in the absence of reflection symmetry [i.e., we have $G^{\mathbb{C}}_{\text{off}}(R^+, s, d) = \pi_0(\mathcal{C}_{s-d+1})$].

2. R_- and R_{--}

Second, we study the case where R anticommutes with all global symmetries. In this case, the reflection operator R can take on three different forms, namely, $R = i\gamma_{d+1}\gamma_{d+2}$, $R = i\tilde{\gamma}_1\tilde{\gamma}_2$, or $R = \mathbb{1} \otimes \sigma_y$. The classification of the gapless Dirac Hamiltonian (C1) can be inferred from the homotopy group $\pi_0(\mathcal{R}_l)$, where $\mathcal{R}_l$ represents the classifying space and $l = s - d + 1 \bmod 8$, with s denoting the symmetry class and d the spatial dimension. Each symmetry class s and dimension d needs to be discussed separately. Since the classification only depends on the difference $s - d$, we discuss it in terms of $l = s - d + 1$. Based on Table IV, we find that for $l = 2,3$ and $l = 5,6$ the reflection operator can be defined as follows:

$$l = 2,3, \quad R = i\gamma_{d+1}\gamma_{d+2}, \tag{C5}$$

$$l = 5,6, \quad R = i\tilde{\gamma}_1\tilde{\gamma}_2. \tag{C6}$$

For $l = 2,3$, we find that there exists an SPGT, i.e., $\sin k_1 \gamma_{d+1}$, which implies trivial topology. Similarly, for $l = 5$, the presence of the symmetry-allowed gap-opening term $i \sin k_1 \tilde{\gamma}_1\tilde{\gamma}_2\tilde{\gamma}_3$ signals trivial topology. For $l = 6$, on the other hand, the Fermi point of Eq. (C1) is stable since there does not exist any SPGT. To distinguish between $\mathbb{Z}_2$ and $\mathbb{Z}$ classifications, we need to consider a doubled version of Hamiltonian (C1) with two identical gapless modes, i.e.,

$$H'_{\text{off}} = H_{\text{off}} \otimes \mathbb{1}. \tag{C7}$$

For $l = 6$, there exists an SPGT $(\sin k_1 \tilde{\gamma}_1 \otimes \sigma_y)$ that can be added to H'_{off}, signaling a $\mathbb{Z}_2$ classification.

For $l = 0,1,7$, it is not possible to implement a reflection symmetry for the minimal Dirac-matrix Hamiltonian (C1). Instead, one needs to consider the doubled version of H_{off}, i.e., Eq. (C7), to study the effects of reflection symmetry. For H'_{off}, reflection symmetry can be implemented as $R = \mathbb{1} \otimes \sigma_y$. For $l = 1$ and 7, SPGTs can be found as $m\tilde{\gamma}_1 \otimes \mathbb{1}$ and $m\gamma_{d+1} \otimes \sigma_y$, respectively. For $l = 0$, however, gap-opening terms are forbidden by symmetry. We find that also for the quadrupled

version of $H_{\rm off}$, i.e.,

$$H''_{\rm off} = H_{\rm off} \otimes \mathbb{1} \otimes \mathbb{1}, \tag{C8}$$

there do not exist any SPGTs in the case of $l = 0$. Therefore, the system exhibits a $2\mathbb{Z}$ classification due to the doubled size of the minimal Hamiltonian (C7).

Finally, for $l = 4$ the system, which corresponds to $2\mathbb{Z}$, can be effectively treated as two identical copies of the $\mathbb{Z}$ system in the spatial dimensions

$$H^{2\mathbb{Z}}_{\rm off} = H^{\mathbb{Z}}_{\rm off} \otimes \mathbb{1}. \tag{C9}$$

The relations of the global symmetry operators between $\mathbb{Z}$ and $2\mathbb{Z}$ are given by $T_{2\mathbb{Z}} = T_{\mathbb{Z}} \otimes \sigma_y$ and $C_{2\mathbb{Z}} = C_{\mathbb{Z}} \otimes \sigma_y$. Therefore, we can simply define $R^- = \mathbb{1} \otimes \sigma_y$, which anticommutes with $T_{2\mathbb{Z}}$ and $C_{2\mathbb{Z}}$. Following the similar discussion of $l = 0$, we find the system of $l = 4$ inherits $\mathbb{Z}$ topology.

3. AIII with R_-, DIII and CI with R_{-+}, and BDI and CII with R_{+-}

Next, we consider class AIII with R_--type reflection symmetry, classes DIII and CI with R_{-+}-type reflection symmetry, and classes BDI and CII with R_{+-}-type reflection symmetry. That is, we have

$$R_- \quad \text{for class AIII,} \tag{C10a}$$

$$R_{+-} \text{ for classes BDI and CII,} \tag{C10b}$$

$$R_{-+} \text{ for classes DIII and CI.} \tag{C10c}$$

In all these cases, there is a chiral symmetry operator S which anticommutes with the Hamiltonian. Using S we can construct the reflection-symmetry operator R as $R = i\gamma_{d+1}S$, where γ_{d+1} represents a kinetic term. Let us clarify how S is related to the two global symmetry operators $T = U_T\mathcal{K}$ and $C = U_C\mathcal{K}$. (Here, we assume that U_T and U_C are Hermitian and unitary.) In general, S is proportional to TC. We choose $S = TC$ if $[U_C^*, U_T] = 0$ and $S = iTC$ if $\{U_C^*, U_T\} = 0$. This choice ensures that R is Hermitian and that R and T/C satisfy the commutation and anticommutation relations of Eqs. (C10b) and (C10c). In order to verify these (anti)commutation relations, one has to make use of Eq. (A1) and the fact that

$$TST^{-1} = \pm S, \quad CSC^{-1} = \pm S, \tag{C11}$$

where we pick up the plus sign in front of S when $T^2 = \pm\mathbb{1}$ and $C^2 = \pm\mathbb{1}$, whereas we pick up the minus sign when $T^2 = \pm\mathbb{1}$ and $C^2 = \mp\mathbb{1}$.

With these definitions, we find that the kinetic term $\sin k_1\gamma_{d+1}$ is an SPGT for all dimensions and all the cases listed in Eq. (C10), i.e., $\sin k_1\gamma_{d+1}$ opens up a full gap and is allowed by both the global symmetries and the reflection symmetry. Hence, for the symmetry classes (C10), the system always has trivial topology. Therefore, we write $G^{\mathbb{R}}_{\rm off}(R^{\mp\pm}, s-d) = 0$ (see Tables V and III).

4. DIII and CI with R_{+-} and BDI and CII with R_{-+}

Last, we discuss classes DIII and CI with R_{+-}-type reflection symmetry and classes BDI and CII with R_{-+}-type reflection symmetry. In a similar way as in the previous subsection, we can construct the reflection operator R in the form of $R = i\tilde{\gamma}_1 S$. This ensures that $\{T, R\} = 0$ and $[C, R] = 0$ when $T^2 = C^2 = \pm\mathbb{1}$; and $[T, R] = 0$ and $\{C, R\} = 0$ when $T^2 = -C^2 = \pm\mathbb{1}$. In the following, we discuss the topology for each symmetry class s and each spatial dimension d separately. Since the classification only depends on the difference $s - d$, we discuss it in terms of $l = s - d + 1$ (cf. Sec. C 2). The classification can also be inferred from the homotopy group $\pi_0(\mathcal{R}_l)$ (cf. Table IV).

TABLE V. Classification of Fermi points outside mirror planes (cf. Table III). The prefix "C" indicates that the $\mathbb{Z}_2$ invariant is defined in terms of the combined symmetries [see Eq. (26)]. The label "$R^{\mp\pm}$" represents R_{-+} for classes BDI and CI; and R_{+-} for classes CI and DIII. Similarly, "$R^{\pm\mp}$" represents R_{+-} for classes BDI and CI; and R_{-+} for classes CI and DIII.

$s-d$	0	1	2	3	4	5	6	7
$G^{\mathbb{R}}_{\rm off}(R^+, s-d)$	$C\mathbb{Z}_2$	$C\mathbb{Z}_2$	0	$2\mathbb{Z}$	0	0	0	$\mathbb{Z}$
$G^{\mathbb{R}}_{\rm off}(R^-, s-d)$	0	0	0	$2\mathbb{Z}$	0	$C\mathbb{Z}_2$	0	$2\mathbb{Z}$
$G^{\mathbb{R}}_{\rm off}(R^{\mp\pm}, s-d)$	0	0	0	0	0	0	0	0
$G^{\mathbb{R}}_{\rm off}(R^{\pm\mp}, s-d)$	0	0	0	0	0	0	$C\mathbb{Z}_2$	$C\mathbb{Z}_2$

For $l = 5, 6$, we find that the reflection operator R can be defined as $R = i\tilde{\gamma}_1 S$, without enlarging the matrix dimension of the minimal Hamiltonian. According to Table IV, there exist at least two mass terms, i.e., $\tilde{\gamma}_1$ and $\tilde{\gamma}_2$, which preserve the global symmetries. The second mass term $\tilde{\gamma}_2$, which preserves also reflection symmetry, gaps out the Fermi points. Hence, the topology is trivial and classified as "0".

For $l = 3$, there exist three kinetic terms γ_{d+1}, γ_{d+2}, and γ_{d+3}, which satisfy Eq. (A1). The product of these three kinetic terms form a mass term $i\gamma_{d+1}\gamma_{d+2}\gamma_{d+3}$, which preserves global symmetries. Hence, the reflection-symmetry operator can be constructed as $R = i\gamma_{d+1}\gamma_{d+2}\gamma_{d+3}S$. The kinetic term $\sin k_1\gamma_{d+1}$, which also preserves reflection symmetry, is allowed to be added to Hamiltonian (C1) as an SPGT. Hence, the case $l = 3$ is classified as the trivial phase.

For $l = 7$, there is only one mass term, namely $\tilde{\gamma}_1$, which is allowed by the global symmetries (see Table IV). So, it is possible to construct the reflection-symmetry operator R as $R = i\tilde{\gamma}_1 S$. The reflection symmetry forbids $\tilde{\gamma}_1$, which is the only term that gaps the Fermi points. Although the Fermi points are stable in the minimal Hamiltonian, to distinguish $\mathbb{Z}_2$ and $\mathbb{Z}$ we have to consider doubled versions of the minimal Hamiltonian. For $H_{\rm off} \otimes \mathbb{1}$, there exists a mass term $\sin k_1\tilde{\gamma}_1 \otimes \sigma_y$ which preserves global symmetries and reflection symmetry with $R = i\tilde{\gamma}_1 S \otimes \mathbb{1}$. Hence, the case $l = 7$ exhibits $\mathbb{Z}_2$ characteristics.

For $l = 1,2$, the reflection operator R for the minimal Hamiltonian (C1) in the absence of the mass term $\tilde{\gamma}_1$ cannot be constructed. In order to study the effects of reflection symmetry, we need to enlarge the matrix dimension and consider two identical copies of $H_{\rm off}$, i.e., $H_{\rm off} \otimes \mathbb{1}$. For $H_{\rm off} \otimes \mathbb{1}$, a mass term can be defined as $\tilde{\gamma}_1 = \gamma_{d+1} \otimes \sigma_y$. Therefore, the reflection-symmetry operator is given by $R = i\gamma_{d+1}S \otimes \sigma_y$. With this, we find that $\gamma_{d+1} \otimes \sigma_x$ is an SPGT that can be added to $H_{\rm off} \otimes \mathbb{1}$. Hence, the case $l = 1,2$ is topologically trivial, i.e., classified as "0".

For $l = 0$, we also need to enlarge the matrix dimension in order to study the effects of reflection symmetry. We consider the following doubled version of Eq. (C1):

$$H_{\text{off}}^{l=0} = \sum_{i=2}^{d} \sin k_i \gamma_i \otimes \mathbb{1} + \left(d - 1 + \sum_{i=1}^{d} \cos k_i \right) \tilde{\gamma}_0 \otimes \sigma_z. \tag{C12}$$

We note that there exist several different doubled versions of H_{off} for which a reflection symmetry can be defined. However, all these different versions are unitarily equivalent, hence, it is sufficient to study only one of them. For Hamiltonian (C12), there exists only one mass term (i.e., $\gamma_0 \otimes \sigma_x$) and one kinetic term (i.e., $\gamma_0 \otimes \sigma_y$) that preserve the global symmetries. The mass term $\gamma_0 \otimes \sigma_x$ can be used to define a reflection operator, i.e., $R = i\tilde{\gamma}_0 S \otimes \sigma_x$. There exist two mass terms which satisfy the global symmetries ($m\tilde{\gamma}_0 \otimes \sigma_x$ and $\sin k_1 \gamma_0 \otimes \sigma_y$). However, these two mass terms break reflection symmetry. Hence, the Fermi points in the case $l = 0$ are topologically stable. To distinguish between $\mathbb{Z}_2$ and $\mathbb{Z}$, the Hamiltonian has to be doubled, i.e, we consider $H_{\text{off}}^{l=0} \otimes \mathbb{1}$. We find that for $H_{\text{off}}^{l=0} \otimes \mathbb{1}$ there exists an SPGT, namely, $m\tilde{\gamma}_0 \otimes \sigma_y \otimes \sigma_y$. Thus, the system is classified as $\mathbb{Z}_2$.

For $l = 4$, a reflection symmetry cannot be implemented for Eq. (C1) (since mass and kinetic terms are absent). We need to consider a quadrupled version of Eq. (C1), in order to study the influence of reflection symmetry. The quadrupled Hamiltonian can be constructed using Eq. (C12). We have

$$H_{\text{off}}^{l=4} = H_{\text{off}}^{l=0} \otimes \mathbb{1}. \tag{C13}$$

The global symmetry operators for this Hamiltonian are given by

$$T^{l=4} = T^{l=0} \otimes \sigma_y, \quad C^{l=4} = C^{l=0} \otimes \sigma_y. \tag{C14}$$

The reflection-symmetry operator can be constructed as $R = i\tilde{\gamma}_0 S \otimes \sigma_x \otimes \mathbb{1}$, where $\tilde{\gamma}_0$ and S are the mass term and the chiral symmetry operator of $H_{\text{off}}^{l=0}$, respectively. We find that the mass term $m\tilde{\gamma}_0 \otimes \sigma_y \otimes \sigma_y$, which preserves the global symmetries and the reflection symmetry, gaps out the Fermi points of $H_{\text{off}}^{l=4}$. Thus, the system is topologically trivial and classified as "0".

[1] M. König, H. Buhmann, L. W. Molenkamp, T. Hughes, C.-X. Liu, X.-L. Qi, and S.-C. Zhang, J. Phys. Soc. Jpn. **77**, 031007 (2008).
[2] M. Z. Hasan and C. L. Kane, Rev. Mod. Phys. **82**, 3045 (2010).
[3] M. Z. Hasan and J. E. Moore, Annu. Rev. Condens. Matter Phys. **2**, 55 (2011).
[4] X.-L. Qi and S.-C. Zhang, Rev. Mod. Phys. **83**, 1057 (2011).
[5] B. A. Bernevig, T. L. Hughes, and S.-C. Zhang, Science **314**, 1757 (2006).
[6] A. Kitaev, AIP Conf. Proc. **1134**, 22 (2009).
[7] A. P. Schnyder, S. Ryu, A. Furusaki, and A. W. W. Ludwig, AIP Conf. Proc. **1134**, 10 (2009).
[8] S. Ryu, A. P. Schnyder, A. Furusaki, and A. W. W. Ludwig, New J. Phys. **12**, 065010 (2010).
[9] A. P. Schnyder, S. Ryu, A. Furusaki, and A. W. W. Ludwig, Phys. Rev. B **78**, 195125 (2008).
[10] J. C. Y. Teo, L. Fu, and C. L. Kane, Phys. Rev. B **78**, 045426 (2008).
[11] L. Fu, Phys. Rev. Lett. **106**, 106802 (2011).
[12] C.-K. Chiu, H. Yao, and S. Ryu, Phys. Rev. B **88**, 075142 (2013).
[13] T. Morimoto and A. Furusaki, Phys. Rev. B **88**, 125129 (2013).
[14] R.-J. Slager, A. Mesaros, V. Juricic, and J. Zaanen, Nat. Phys. **9**, 98 (2013).
[15] Y. Ueno, A. Yamakage, Y. Tanaka, and M. Sato, Phys. Rev. Lett. **111**, 087002 (2013).
[16] F. Zhang, C. L. Kane, and E. J. Mele, Phys. Rev. Lett. **111**, 056403 (2013).
[17] W. A. Benalcazar, J. C. Y. Teo, and T. L. Hughes, Phys. Rev. B **89**, 224503 (2014).
[18] C. Fang, M. J. Gilbert, and B. A. Bernevig, Phys. Rev. B **86**, 115112 (2012).
[19] C. Fang, M. J. Gilbert, and B. A. Bernevig, Phys. Rev. B **87**, 035119 (2013).
[20] P. Jadaun, D. Xiao, Q. Niu, and S. K. Banerjee, Phys. Rev. B **88**, 085110 (2013).
[21] J. C. Y. Teo and T. L. Hughes, Phys. Rev. Lett. **111**, 047006 (2013).
[22] A. M. Turner, Y. Zhang, R. S. K. Mong, and A. Vishwanath, Phys. Rev. B **85**, 165120 (2012).
[23] A. M. Turner, Y. Zhang, and A. Vishwanath, Phys. Rev. B **82**, 241102 (2010).
[24] T. L. Hughes, E. Prodan, and B. A. Bernevig, Phys. Rev. B **83**, 245132 (2011).
[25] Y.-M. Lu and D.-H. Lee, arXiv:1403.5558.
[26] K. Shiozaki and M. Sato, Phys. Rev. B **90**, 165114 (2014).
[27] M. Koshino, T. Morimoto, and M. Sato, Phys. Rev. B **90**, 115207 (2014).
[28] Y. Tanaka, Z. Ren, T. Sato, K. Nakayama, S. Souma, T. Takahashi, K. Segawa, and Y. Ando, Nat Phys **8**, 800 (2012).
[29] T. H. Hsieh, H. Lin, J. Liu, W. Duan, A. Bansil, and L. Fu, Nat. Commun. **3**, 982 (2012).
[30] S.-Y. Xu, C. Liu, N. Alidoust, M. Neupane, D. Qian, I. Belopolski, J. D. Denlinger, Y. J. Wang, H. Lin, L. A. Wray *et al.*, Nat. Commun. **3**, 1192 (2012).
[31] P. Dziawa, B. J. Kowalski, K. Dybko, R. Buczko, A. Szczerbakow, M. Szot, E. Łusakowska, T. Balasubramanian, B. M. Wojek, M. H. Berntsen, O. Tjernberg, and T. Story, Nat. Mater. **11**, 1023 (2012).
[32] S. Ryu and Y. Hatsugai, Phys. Rev. Lett. **89**, 077002 (2002).
[33] S. Matsuura, P.-Y. Chang, A. P. Schnyder, and S. Ryu, New J. Phys. **15**, 065001 (2013).
[34] Y. X. Zhao and Z. D. Wang, Phys. Rev. Lett. **110**, 240404 (2013).
[35] Y. X. Zhao and Z. D. Wang, Phys. Rev. B **89**, 075111 (2014).
[36] P. Hořava, Phys. Rev. Lett. **95**, 016405 (2005).
[37] B. Béri, Phys. Rev. B **81**, 134515 (2010).
[38] G. E. Volovik, *Universe in a Helium Droplet* (Oxford University Press, Oxford, UK, 2003).
[39] G. E. Volovik, *Topology of Quantum Vacuum*, Vol. 870 of Lecture Notes in Physics (Springer, Berlin, 2013).
[40] J. L. Mañes, Phys. Rev. B **85**, 155118 (2012).
[41] A. Lau and C. Timm, Phys. Rev. B **88**, 165402 (2013).
[42] Y. Ran, F. Wang, H. Zhai, A. Vishwanath, and D.-H. Lee, Phys. Rev. B **79**, 014505 (2009).
[43] J.-M. Hou, Phys. Rev. Lett. **111**, 130403 (2013).

[44] S. Kobayashi, K. Shiozaki, Y. Tanaka, and M. Sato, Phys. Rev. B **90**, 024516 (2014).

[45] A. A. Burkov, M. D. Hook, and L. Balents, Phys. Rev. B **84**, 235126 (2011).

[46] A. A. Burkov and L. Balents, Phys. Rev. Lett. **107**, 127205 (2011).

[47] X. Wan, A. M. Turner, A. Vishwanath, and S. Y. Savrasov, Phys. Rev. B **83**, 205101 (2011).

[48] C. Fang, M. J. Gilbert, X. Dai, and B. A. Bernevig, Phys. Rev. Lett. **108**, 266802 (2012).

[49] P. Delplace, J. Li, and D. Carpentier, Europhys. Lett. **97**, 67004 (2012).

[50] L. Lu, L. Fu, J. D. Joannopoulos, and M. Soljacic, Nat. Photonics **7**, 294 (2013).

[51] G. Xu, H. Weng, Z. Wang, X. Dai, and Z. Fang, Phys. Rev. Lett. **107**, 186806 (2011).

[52] T. Das, Phys. Rev. B **88**, 035444 (2013).

[53] V. Shivamoggi and M. J. Gilbert, Phys. Rev. B **88**, 134504 (2013).

[54] P. K. Biswas, H. Luetkens, T. Neupert, T. Stürzer, C. Baines, G. Pascua, A. P. Schnyder, M. H. Fischer, J. Goryo, M. R. Lees *et al.*, Phys. Rev. B **87**, 180503 (2013).

[55] M. H. Fischer, T. Neupert, C. Platt, A. P. Schnyder, W. Hanke, J. Goryo, R. Thomale, and M. Sigrist, Phys. Rev. B **89**, 020509 (2014).

[56] T. Meng and L. Balents, Phys. Rev. B **86**, 054504 (2012).

[57] J. D. Sau and S. Tewari, Phys. Rev. B **86**, 104509 (2012).

[58] M. Sato, Phys. Rev. B **73**, 214502 (2006).

[59] A. P. Schnyder and S. Ryu, Phys. Rev. B **84**, 060504 (2011).

[60] P. M. R. Brydon, A. P. Schnyder, and C. Timm, Phys. Rev. B **84**, 020501 (2011).

[61] F. Wang and D.-H. Lee, Phys. Rev. B **86**, 094512 (2012).

[62] A. P. Schnyder, P. M. R. Brydon, and C. Timm, Phys. Rev. B **85**, 024522 (2012).

[63] Y. Tanaka, M. Sato, and N. Nagaosa, J. Phys. Soc. Jpn. **81**, 011013 (2012).

[64] P. M. R. Brydon, C. Timm, and A. P. Schnyder, New J. Phys. **15**, 045019 (2013).

[65] A. P. Schnyder, C. Timm, and P. M. R. Brydon, Phys. Rev. Lett. **111**, 077001 (2013).

[66] A. Altland and M. R. Zirnbauer, Phys. Rev. B **55**, 1142 (1997).

[67] M. R. Zirnbauer, J. Math. Phys. **37**, 4986 (1996).

[68] Z. Wang, X.-L. Qi, and S.-C. Zhang, Phys. Rev. Lett. **105**, 256803 (2010).

[69] H. Nielsen and M. Ninomiya, Nucl. Phys. B **185**, 20 (1981).

[70] A. M. Essin and V. Gurarie, Phys. Rev. B **84**, 125132 (2011).

[71] L. Fu and C. L. Kane, Phys. Rev. B **74**, 195312 (2006).

[72] P.-Y. Chang, S. Matsuura, A. P. Schnyder, and S. Ryu, Phys. Rev. B **90**, 174504 (2014).

[73] M. Stone, C.-K. Chiu, and A. Roy, J. Phys. A: Math. Theor. **44**, 045001 (2011).

[74] C.-K. Chiu, arXiv:1410.1117.

[75] T. Morimoto and A. Furusaki, Phys. Rev. B **89**, 235127 (2014).

[76] Since the topological invariant cannot change as a function of k_1 as long as the bulk gap does not close, the invariant defined in the mirror plane must equal the invariant defined in a plane that is perpendicular to k_1 and infinitesimally close to the mirror plane. Due to this condition, the "stronger" of the two invariants reduces to the "weaker" one.

[77] The distinction between $\mathbb{Z}$ and $2\mathbb{Z}$ classification follows from the Dirac-matrix Hamiltonian approach.

[78] Note that this model is similar to the BHZ model describing the quantum spin Hall effect in HgTe quantum wells [1,4,5].

[79] A. H. Castro Neto, F. Guinea, N. M. R. Peres, K. S. Novoselov, and A. K. Geim, Rev. Mod. Phys. **81**, 109 (2009).

[80] A. Kitaev, Phys.-Usp. **44**, 131 (2000).

[81] L. Fu and C. L. Kane, Phys. Rev. B **76**, 045302 (2007).

[82] T. Ojanen, Phys. Rev. B **87**, 245112 (2013).

[83] S. M. Young, S. Zaheer, J. C. Y. Teo, C. L. Kane, E. J. Mele, and A. M. Rappe, Phys. Rev. Lett. **108**, 140405 (2012).

[84] J. A. Steinberg, S. M. Young, S. Zaheer, C. L. Kane, E. J. Mele, and A. M. Rappe, Phys. Rev. Lett. **112**, 036403 (2014).

[85] Z. K. Liu, B. Zhou, Y. Zhang, Z. J. Wang, H. M. Weng, D. Prabhakaran, S.-K. Mo, Z. X. Shen, Z. Fang, X. Dai *et al.*, Science **343**, 864 (2014).

[86] M. Neupane, S.-Y. Xu, R. Sankar, N. Alidoust, G. Bian, C. Liu, I. Belopolski, T.-R. Chang, H.-T. Jeng, H. Lin, A. Bansil, F. Chou, and M. Z. Hasan, Nat. Commun. **5**, 3786 (2014).

[87] Z. Wang, Y. Sun, X.-Q. Chen, C. Franchini, G. Xu, H. Weng, X. Dai, and Z. Fang, Phys. Rev. B **85**, 195320 (2012).

[88] S. Jeon, B. B. Zhou, A. Gyenis, B. E. Feldman, I. Kimchi, A. C. Potter, Q. D. Gibson, R. J. Cava, A. Vishwanath, and A. Yazdani, Nat. Mater. **13**, 851 (2014).

[89] Z. Wang, H. Weng, Q. Wu, X. Dai, and Z. Fang, Phys. Rev. B **88**, 125427 (2013).

[90] Z. K. Liu, J. Jiang, B. Zhou, Z. J. Wang, Y. Zhang, H. M. Weng, D. Prabhakaran, S.-K. Mo, H. Peng, P. Dudin *et al.*, Nat. Mater. **13**, 677 (2014).

[91] Note that the Chern or winding number of the $R = -1$ and $+1$ sectors only differ by a minus sign, as long as the Chern or winding number of the entire Hamiltonian $H(\mathbf{k})|_{k_l=0,\pi}$ (i.e., both blocks together) is vanishing.

[92] Note that the edge Hamiltonian $h^{\mathrm{CII}}_{\mathrm{edge}}$ and the symmetry operators T_{edge}, C_{edge}, and R_{edge} are only defined up to a similarity transformation since one is free to choose a basis among the degenerate states of the Hamiltonian. The topological properties, however, are independent of this basis choice.